PERFORMANCE MEASURES FOR OSCILLATOR NETWORKS

by

Theodore W. Grunberg

An essay submitted to The Johns Hopkins University in conformity with the requirements for the degree of Master of Science in Engineering.

Baltimore, Maryland

May, 2015

Abstract

Oscillator networks consist of a set of simple subsystems, e.g. damped harmonic oscillators that interact with each other across a network with a specified structure. Such networks of coupled oscillators serve as a model for many systems such as power grids, vehicle platoons, and biological networks. Even though the dynamics of each oscillator are simple, the coupling between them can produce complex behavior. One possible behavior is synchronization, where all of the oscillators reach a state where their relative phase angles are constant and their frequencies are uniform. This work examines the synchronization performance of oscillator networks, i.e. how well the network maintains synchrony in the face of persistent disturbances. Specifically, we define a class of performance measures for oscillator networks as the $\mathcal{H}_2$-norm of particular input-output linear systems. This class of performance measures corresponds to measuring the average value of a quadratic form of the oscillator phases when stochastic disturbances are applied to some subset of the oscillators. Depending on the specific quadratic form that is chosen, this performance measure can correspond to a variety of physically meaningful and domain specific quantities. For example,

ABSTRACT

it can be used to quantify the total interactions between oscillators during resynchronization after a disturbance. This quantity corresponds to the transient resistive losses in maintaining synchronous operation in a power network. Alternatively, one can instead measure the network coherence, which quantifies how closely the oscillator network acts like a single rigid body. Our results demonstrate a strong connection between the concept of effective resistance and our class of performance measures. For example, our results make precise the intuitive notion that more "tightly connected" oscillator networks are more coherent by showing that the maximum effective resistance in the network is the correct notion of connectivity. We consider applications of the work to both power grids and vehicle platoons with local and absolute (global) velocity feedback. For power grids we use our effective resistance based results to obtain novel bounds on the resistive losses due to generators maintaining synchrony. For vehicle platoons we investigate the coherence in the platoon as a performance measure. We show that for large scale platoons local velocity feedback performs worse than absolute velocity feedback under certain conditions related to the asymptotic behavior of the maximum effective resistance in the underlying graph.

Primary Reader: Dennice F. Gayme

Secondary Reader: Noah J. Cowan

Acknowledgments

I would like to thank my advisor, Professor Dennice F. Gayme, for her constant mentoring and encouragement during my masters studies at JHU. Not only have I enjoyed working with her, but I have also gained an appreciation for research through her enthusiastic example.

I would also like to thank Professor Noah J. Cowan for generously serving as the second reader for this essay, and for his helpful comments on the same.

Additionally, I would like to thank Emma Tegling (née Sjödin) for several insightful discussions that greatly enhanced this work. Finally, financial support from NSF grant number ECCS 1230788 is also gratefully acknowledged.

Contents

List of Tables

List of Figures

Chapter 1

Introduction

Oscillator networks can be used to model a wide variety of problems ranging from vehicle platoons [1–3] and power grids [4–7] to chemical and biological networks [8]. An important question that is often investigated is whether a set of coupled oscillators will synchronize, or reach some stable operating condition where the relative phases of all the oscillators are constant. An overview of results pertaining to synchronization of oscillator networks is provided in [9].

A number of researchers have recently investigated the related but equally important question of how oscillators reach or maintain a synchronous state, i.e. the synchronization performance. The performance of oscillator networks can be quantified in a variety of ways, such as the total interactions between oscillator, the network disorder, or the speed of convergence. Most of these performance measures quantify how the network behaves when stochastic disturbances are applied to every oscillator, for linear oscillator networks a large class of such performance measures can be computed as the $\mathcal{H}_2$-norm of an appropriately defined linear system. For example, Young et al. [10] use an $\mathcal{H}_2$-norm based performance measure to study the performance of consensus dynamics being forced by noise. Siami and Motee [11] use a similar notion to investigate graph theoretic limits on the performance of oscillator networks subjected to stochastic disturbances. Tegling et al. [12] use such a measure to quantify the transient real power losses in power networks incurred in maintaining synchrony. These additional real power losses are due to the generator phases deviating from their nominal values. These deviations in phase angles cause additional power to be circulate among the generators, which leads to real power losses due to the power flowing between the generators. Dörfler et al. [13] study minimizing the $\mathcal{H}_2$-norm of an oscillator network by using wide-area control to prevent inter-area oscillations while simultaneously promoting sparsity in the controller. Additionally, Lin et al. [14] studied $\mathcal{H}_2$-norm minimizing control for vehicle platoons with a line structure.

Another performance measure that has been studied is coherence. In the context of oscillator networks, coherence is the degree to which a set of oscillators behaves like a rigid body, for example a group of vehicles forming a rigid structure. Coherence can be thought of as both a performance measure and a form of stability. Coherence can be used as a performance measure in that it can be used to measure how closely the network follows some desired behavior. Coherence is also often related to stability because it measures how far from the state of the network is from the equilibrium point, and thus how likely the network is to leave the region of attraction of an asymptotically stable equilibrium point. Bamieh et al. [15] investigated the scaling of coherence with graph dimension d in vehicle platoons distributed over toroidal graphs. In particular, they showed that the asymptotic scaling of the network's coherence is much worse when each vehicle has access to only local velocity or position feedback rather than the global or absolute measures of these quantities when the dimension of the torus is small.

The behavior of oscillator networks can also be evaluated based on properties of the underlying graph. The effective resistance, for example, is a quantity defined for any two nodes in a weighted graph. It is a metric on the vertex set, and corresponds to the electrical resistance between two nodes in a resistor network with the same structure as the graph. This concept has been used to characterize both stability and performance in a large range of applications, including oscillator and consensus networks. Dörfler and Bullo [16] obtained conditions for synchronization in power networks in terms of effective resistance. Barooah and Hespanha [17] related the stability of vehicle formations to the effective resistance of the underlying graph. They also found that the error in estimating quantities from relative measurements is strongly related to the notion of effective resistance [18]. The results that we present in this work connect the performance of oscillator networks to the effective resistance between vertices in the underlying graphs. This yields closed form expressions for the the network performance that have both a physical interpretation and can in many cases be easily computed by hand.

The previously described works quantify the performance of the network in a global sense by applying disturbances to all of the oscillators and measuring the response of the entire network. In contrast, Huang et. al. [19] studied the performance of networks of first order systems by considering the steady state variance of particular nodes under the effect of disturbances at every node. In this work we investigate a novel spatially local class of performance measures. In particular these measures allow us to isolate a subset of the network to evaluate its performance. We compute these measures by first deriving mathematics to extend Gramian computations to non-minimal realizations. We therefore do not need to rely on Fourier analysis as in previous results, e.g. [15] which allows us to expand our analysis from locally compact Abelian groups to more general graphs. We apply our performance measures to networks with local and global damping, which respectively refer to the oscillators being damped either relative to their absolute frequencies, or their frequencies relative to their neighbors.

The remainder of this essay is organized as follows. Chapter 2 describes the notation and provides some mathematical background material. In Chapter 3 we introduce the system models that we study in this work.

Chapter 4 provides the first theoretical results. These results provide methods to compute the observability Gramian for non-minimal realizations of systems on graphs. To do this, we extend Lyapunov equation theory to unstable realizations that are bounded-input bounded-output (BIBO) stable. We then derive closed form expressions for the observability Gramian for a particular class of systems, which includes the oscillator networks presented in Chapter 3. These results allow us to compute the $\mathcal{H}_2$-norms of a large class of systems on graphs.

Chapter 5 makes use of the theory developed in Chapter 4 to develop the main results. We first consider the behavior of oscillator networks when a disturbance is applied at a single location in the network. We then use the Gramian expressions developed in Chapter 4 to relate both the network's coherence as well as the total interaction between oscillators to the effective resistance in the underlying graphs. We then consider the case of disturbances applied at every oscillator in the network, and define the nodal performance of a pair of oscillators in the network. This nodal performance describes the steady state variance between the phases of the two nodes considered. If the two oscillators are adjacent, their nodal performance quantifies how much they interact to maintain synchrony. If they are far apart in the network, their nodal performance measures the coherence of the network or a subset of it in terms of long range disorder [15]. We relate the nodal performance to the effective resistances of the underlying graphs, and then show how the nodal performance of different pairs of oscillators in the network can be combined to construct a large class of performance measures. By analytically computing the effective resistance for several specific graph structures we derive detailed results that provide insight into the asymptotic performance of large scale oscillator networks. Finally, we provide a graph theoretic proof that the effective resistance between any two nodes connected by a single path depends only on the properties of the graph along the connecting path. This result can be used to illustrate the qualitative differences between oscillator networks with local and global damping. Chapter 6 applies our results to power grids and vehicle platoons, and includes numerical studies for these interesting applications.

The main contributions of this work are as follows. First, we provide a systematic study of computing the $\mathcal{H}_2$-norms of oscillator networks directly from the standard, non-minimal realization. Second, we provide results for the performance of oscillator networks with localized disturbances as well as for networks with distributed disturbances, but with performance measured pairwise. Third, we show the strong connection between the performance of oscillator networks and effective resistance. Finally, we give results evaluating the transient power losses in power grids near a non-zero synchronous state. This is in contrast to previous work such as [20] and [21] which considered only synchronous states where the nominal power flows are all zero.

Chapter 2

Mathematical Preliminaries

This chapter introduces the notation that is used throughout this work, and additionally presents mathematical background material that will be used later.

2.1 Notation

Unless other wise noted, we denote vectors, matrices respectively by bold symbols ($\mathbf{a} \in \mathbb{R}^n$) and capital letters ($A$). Given $A \in \mathbb{R}^{n\times n}$, $A < 0$ [$A > 0$] and $A \leq 0$ [$A \geq 0$] denote that A is symmetric and respectively negative [positive] definite and negative [positive] semi-definite.

Given two vector spaces, V and W, such that $V \subseteq W$, $V^\perp$ denotes the orthogonal complement of V in W. For $V \subseteq \mathbb{R}^n$, $V^\perp$ denotes the othogonal complement of V in $\mathbb{R}^n$ unless otherwise specified.

Given $A, B \in \mathbb{C}^{n\times m}$ we denote the transpose and complex conjugate transpose of A by $A^\intercal$ and A^* respectively. Additionally, the Frobenius inner product of A and B is denoted by $\langle A, B\rangle_F := \operatorname{tr}(B^* A)$, and the associated Frobenius norm of A is denoted by $\|A\|_F := \langle A, A\rangle_F$.

$\mathcal{L}_2^n$ denotes the n dimensional complex valued Lebesgue space. Given $x, y \in \mathcal{L}_2^n$, $\langle x, y\rangle_{\mathcal{L}_2} := \int_0^\infty y(\tau)^* x(\tau)\, d\tau$.

$J \in \mathbb{R}^{n\times n}$ denotes the n by n matrix where every element is 1. $I \in \mathbb{R}^{n\times n}$ denotes the n by n identity matrix.

2.2 Moore-Penrose Pseudoinverse

We will make extensive use of the Moore-Penrose pseudoinverse in this work, as so here we state its formal definition. Let $A \in \mathbb{R}^{n\times m}$. A Moore-Penrose pseudoinverse of A is a matrix, $A^\dagger \in \mathbb{R}^{m\times n}$, such that

1. $AA^\dagger A = A$
2. $A^\dagger A A^\dagger = A^\dagger$
3. $\left(AA^\dagger\right)^* = AA^\dagger$
4. $\left(A^\dagger A\right)^* = A^\dagger A.$

It is true that such a $A^\dagger$ always exists and is unique. Therefore we refer to $A^\dagger$ as *the* Moore-Penrose pseudoinverse of A.

It will be useful for us to extend this definition to linear operators between matrices. We do this as follows. Let $L : \mathbb{C}^{n\times m} \to \mathbb{C}^{p\times q}$. A Moore-Penrose pseudoinverse of L is a linear operator, $L^\dagger : \mathbb{C}^{p\times q} \to \mathbb{C}^{n\times m}$, such that

1. $LL^\dagger L = L$
2. $L^\dagger L L^\dagger = L^\dagger$
3. $\left(LL^\dagger\right)^* = LL^\dagger$
4. $\left(L^\dagger L\right)^* = L^\dagger L$

where $\left(LL^\dagger\right)^*$ denotes the adjoint of $LL^\dagger$ using the Frobenius inner product. i.e. $\left(LL^\dagger\right)^* : \mathbb{C}^{n\times m} \to \mathbb{C}^{n\times m}$ is the linear operator that satisfies

$$\left\langle LL^\dagger X, Y\right\rangle_F = \left\langle X, \left(LL^\dagger\right)^* Y\right\rangle_F, \forall X, Y \in \mathbb{C}^{n\times m}. \tag{2.1}$$

As in the case of matrices, $L^\dagger$ always exists and is unique.

2.3 Graph Theory

This sections describes the basic notions from graph theory that we will use to efficiently describe the interconnection structure of oscillator networks.

An undirected, weighted, graph, Γ, is defined as a triple, $\Gamma = (\mathcal{V}, \mathcal{E}, \mathcal{W})$ where $\mathcal{V}$, $\mathcal{E}$, and $\mathcal{W}$ are respectively the vertex set, edge set and weighting function. In this work we assume that $\mathcal{V} = \{1, \ldots, n\}$ where n is the number of vertices. $\mathcal{E}$ is a set of unordered pairs of elements of $\mathcal{V}$, called the edges of Γ, i.e. each element of $\mathcal{E}$ is of the form $\{i, j\}$, $i, j \in \mathcal{V}$. $\mathcal{W}$ is a map that assigns an edge weight to each element of $\mathcal{E}$, i.e. $\mathcal{W} : \mathcal{E} \to \mathbb{R}$. By a slight abuse of notation we write that $\mathcal{W}(\{i, j\}) := 0$, $\forall \{i, j\} \notin \mathcal{E}$. The weighted adjacency matrix, $A \in \mathbb{R}^{n \times n}$ associated with Γ is defined as

$$[A]_{ij} := \mathcal{W}(\{i, j\}). \tag{2.2}$$

The weighted graph Laplacian, L_Γ, of a graph, Γ is defined as

$$L_\Gamma := \operatorname{diag}(A\mathbf{1}) - A. \tag{2.3}$$

A directed weighted graph, Γ' is defined as $\Gamma' = (\mathcal{V}', \mathcal{E}', \mathcal{W}')$, where as in the undirected case $\mathcal{V}' = \{1, \ldots, n\}$ is the vertex set. $\mathcal{E}'$ is the edge set which is composed of ordered pairs of elements of $\mathcal{V}'$, e.g. $(i, j) \in \mathcal{E}'$, $i, j \in \mathcal{V}'$. $\mathcal{W}' : \mathcal{E}' \to \mathbb{R}$ is the weighting function. As in the undirected case we use the convention that $\mathcal{W}'((i, j)) := 0$, $\forall (i, j) \notin \mathcal{E}'$.

Given an undirected weighted graph, $\Gamma = (\mathcal{V}, \mathcal{E}, \mathcal{W})$, an orientation of Γ is any directed, weighted graph, $\Gamma' = (\mathcal{V}', \mathcal{E}', \mathcal{W}')$, such that $\mathcal{V} = \mathcal{V}'$, $\forall \{i, j\} \in \mathcal{E}$ either $(i, j) \in \mathcal{E}'$ or $(j, i) \in \mathcal{E}'$ but not both, and $\mathcal{W}'((i, j)) = \mathcal{W}(\{i, j\})$, $\forall)i, j) \in \mathcal{E}'$.

An unweighted graph, Γ is a pair, $\Gamma = (\mathcal{V}, \mathcal{E})$ where $\mathcal{V} = \{1, \ldots, n\}$ $\mathcal{V}$ is the vertex set and the edge set, $\mathcal{E}$, is either the same as in an undirected weighted graph, in which case Γ is undirected, or the same as in a directed weighted graph, in which case Γ is directed. The adjacency matrix, $A \in \mathbb{R}^{n\times n}$ of Γ is defined as

$$[A]_{ij} := \begin{cases} 1 & \{i,j\} \in \mathcal{E} \\ 0 & \text{otherwise} \end{cases} \tag{2.4}$$

The graph Laplacian, $L_\Gamma \in \mathbb{R}^{n\times n}$ of Γ is defined as

$$[L_\Gamma]_{ij} := \operatorname{diag}(A\mathbf{1}) - A. \tag{2.5}$$

In this work we will mainly deal with the [weighted] adjacency matrices and [weighed] graph Laplacians, it is sufficient for our purposes to consider an unweighted graph as a weighted graph where $\mathcal{W}(a) = 1$, $\forall a \in \mathcal{E}$.

Given a graph, $\Gamma = (\mathcal{V}, \mathcal{E}, \mathcal{W})$, we define a path, $\mathcal{P}$, as a sequence of vertices of Γ, $\mathcal{P} = (p_1, \ldots, p_m, p_{m+1}), p_i \in \mathcal{V}$, $\forall 1 \leq i \leq m+1$, where $\{p_i, p_{i+1}\} \in \mathcal{E}$, $\forall 1 \leq i \leq m$ and $p_i \neq p_j$, $\forall 1 \leq i < j \leq m+1$. We define the length of the path as the number of edges it traverses, m.

2.3.1 Factorizations of the weighted graph Laplacian

Here we give several factorizations of the weighted graph Laplacian which will be used in this work. We begin by giving the definition of the standard oriented incidence matrix, M, which has the property $M^\intercal M = L_\Gamma$ for unweighted graphs. We then define two related matrices that can be used to decompose the weighted graph Laplacian in similar ways.

An oriented incidence matrix, $M \in \mathbb{R}^{|\mathcal{E}|\times|V|}$, of an undirected graph, Γ, is defined as

$$[M]_{lj} := \begin{cases} -1, & \varepsilon_l = (i,j) \\ 1, & \varepsilon_l = (j,i) \\ 0, & \text{otherwise} \end{cases} \tag{2.6}$$

Where $\Gamma' = (\mathcal{V}, \mathcal{E}', \mathcal{W})$ is an orientation of Γ and the elements of $\mathcal{E}'$ are labeled such that $\mathcal{E}' = \left\{\varepsilon_1, \ldots, \varepsilon_{|\mathcal{E}|}\right\}$. If $\mathcal{W} = 1$, $\forall \{i,j\} \in \mathcal{E}$, $M^\intercal M = L_\Gamma$.

By analogy with an oriented incidence matrix of an unweighted graph, we define a weighted, oriented, incidence matrix of the undirected graph Γ as follows. Assume that $\mathcal{W}(\{i,j\}) > 0$, $\forall \{i,j\} \in \mathcal{E}$. The weighted, oriented incidence matrix, $M_W \in \mathbb{R}^{|\mathcal{E}|\times|V|}$ is

$$[M_W]_{lj} := \begin{cases} -\sqrt{\mathcal{W}(\{i,j\})}, & \varepsilon_l = (i,j) \\ \sqrt{\mathcal{W}(\{i,j\})}, & \varepsilon_l = (j,i) \\ 0, & \text{otherwise} \end{cases} \tag{2.7}$$

Where ε_l is the l^{th} element of $\mathcal{E}$. It is easy to show that $M_W^\intercal M_W = L_\Gamma$. When $\mathcal{W}(\{i,j\}) = 1$ for all $\{i,j\} \in \mathcal{E}$ M_W reduces to the usual oriented incidence matrix.

Finally we remark that since L_Γ is positive semi-definite, $L_\Gamma^{\frac{1}{2}}$ exists and so we have $L_\Gamma = L_\Gamma^{\frac{1}{2}} L_\Gamma^{\frac{1}{2}}$.

2.3.2 Effective resistance

Effective resistance is a quantity defined for any pair of vertices in an undirected graph. We state the definition of effective resistance and then give the physical intuition behind it, which comes from circuit theory.

Definition 1. Consider an undirected, weighted graph $\Gamma = (\mathcal{V}, \mathcal{E}, \mathcal{W})$. The effective resistance between vertices i and j in Γ, $R_{\Gamma ij}$, is defined as

$$R_{\Gamma ij} := (\mathbf{e}_i - \mathbf{e}_j)^\intercal L_\Gamma^\dagger (\mathbf{e}_i - \mathbf{e}_j) . \tag{2.8}$$

Consider a resistor network represented by Γ where $\mathcal{V}$ is the set of nodes and $\mathcal{W}(\{i, j\})$ is the susceptance of the resistor connecting nodes i and j. If we inject one amp of current at node i while removing one amp of current at node j, $V_i - V_j = R_{\Gamma ij}$ where $V_i - V_j$ is the voltage difference between nodes i and j. [16]

2.4 $\mathcal{H}_2$-norm

In this section we give the definition of the $\mathcal{H}_2$-norm of a linear system, review the standard method of computing the $\mathcal{H}_2$-norm algebraically, and give three interpretations of the $\mathcal{H}_2$-norm.

Given a bounded-input bounded-output (BIBO) stable linear system, G, the $\mathcal{H}_2$-

norm of G, $\|G\|_{\mathcal{H}_2}$, is defined as

$$\|G\|_{\mathcal{H}_2} := \left(\frac{1}{2\pi}\int_{-\infty}^{\infty}\|G(j\omega)\|_F^2 d\omega\right)^{\frac{1}{2}} \tag{2.9}$$

where $G(j\omega)$ is the frequency response matrix of G.

2.4.1 Computing the $\mathcal{H}_2$-norm

Given a bounded-input bounded-output (BIBO) stable linear system G, and a minimal realization of G, $\hat{G} := \left(\begin{array}{c|c} A & B \\ \hline C & 0 \end{array}\right)$, there are well known algebraic formulas for $\|G\|_{\mathcal{H}_2}$. $\|G\|_{\mathcal{H}_2}$ can be computed using the observability Gramian, X, of $\hat{G}$ as

$$\|G\|_{\mathcal{H}_2} = \sqrt{\operatorname{tr}(B^{\intercal}XB)}, \tag{2.10}$$

where X is the unique positive definite solution to the Lyapunov equation

$$A^{\intercal}X + XA = -C^{\intercal}C. \tag{2.11}$$

Alternatively, $\|G\|_{\mathcal{H}_2}$ can be computed using the controllability Gramian, P, of $\hat{G}$ as

$$\|G\|_{\mathcal{H}_2} = \sqrt{\operatorname{tr}(CPC^{\intercal})}, \tag{2.12}$$

where P is the unique positive definite solution to the Lyapunov equation

$$A^{\mathsf{T}}P + PA = -BB^{\mathsf{T}}. \tag{2.13}$$

When $\hat{G}$ is a non-minimal realization of G, one must first find a minimal realization of G before using one of the two above methods for computing $\|G\|_{\mathcal{H}_2}$. However, for systems where we have a physically meaningful but non-minimal realization it can be advantageous to compute the $\mathcal{H}_2$ norm directly from the non-minimal realization. One instance where this is the case is often the case is systems distributed over graphs. In Chapter 4 we present results that allow us to compute the Gramians of certain classes of systems that correspond to systems distributed over graphs.

2.4.2 Interpretations of the $\mathcal{H}_2$-norm

The $\mathcal{H}_2$-norm is commonly used to measure the performance of linear systems. It measures the aggregate performance of the system

Response to stochastic forcing If the inputs to G are independent white noise with unit strength,

$$\|G\|_{\mathcal{H}_2} = \sqrt{\lim_{t\to\infty} E\left[\mathbf{y}^{\mathsf{T}}\mathbf{y}\right]},$$

where $\mathbf{y}$ is the output of G. Therefore the $\mathcal{H}_2$-norm measures the expected steady state power of the output under stochastic forcing.

Response to random initial conditions Consider the output of $\hat{G}$ with initial conditions $\mathbf{x}_0$. If $\mathbf{x}_0$ is a random variable with $\mathbf{x}_0 \sim \mathcal{N}\left(0, BB^\intercal\right)$,

$$\|G\|_{\mathcal{H}_2} = \sqrt{E\left[\int_0^\infty \mathbf{y}^\intercal \mathbf{y} dt\right]}.$$

Here $\mathbf{x}_0 \sim \mathcal{N}\left(0, BB^\intercal\right)$ denotes that the random variable $\mathbf{x}_0$ is normally distributed with zero mean and covariance $BB^\intercal$. Hence the $\mathcal{H}_2$-norm measures the average autonomous response of G.

Sum of responses to impulses Let $\mathbf{y}_i$ be the output of G when the input is $\delta\left(t\right)\mathbf{e}_i \in \mathbb{R}^m$. Then

$$\|G\|_{\mathcal{H}_2} = \sqrt{\sum_{i=1}^{m} \int_0^\infty \mathbf{y}_i^\intercal \mathbf{y}_i dt}.$$

This deterministic interpretation of the $\mathcal{H}_2$-norm shows that the $\mathcal{H}_2$-norm measures the aggregate impulse response of G, in the sense that it is equal to the sum of all the responses where an impulse is applied to one of the inputs.

Chapter 3

Oscillator Network Models

Oscillator networks provide a model for many systems consisting of multiple simple subsystems connected together. In this chapter we introduce the oscillator network models that we study in this work. We begin by introducing a general oscillator network model. We then present three special cases that correspond to oscillator networks with important applications.

3.1 General Oscillator Network

We consider a network consisting of n coupled oscillators. The coupling between oscillators is described by two graphs, $\mathcal{B} = (\mathcal{V}, \mathcal{E}_B, \mathcal{W}_B)$ and $\mathcal{D} = (\mathcal{V}, \mathcal{E}_D, \mathcal{W}_D)$ where each oscillator is associated with an element of $\mathcal{V}$. By abuse of notation we refer to the oscillators by the vertex they are associated with, i.e. "oscillator i" is the oscillator associated with $i \in \mathcal{V}$. $\mathcal{B}$ describes the position based coupling between oscillators and $\mathcal{D}$ describes the velocity based coupling between oscillators. We assume that $\mathcal{B}$ and $\mathcal{D}$ are connected. The dynamics of the i^{th} oscillator are then given by

$$m\ddot{x}_i + \beta\dot{x}_i + \sum_{\{i,j\}\in\mathcal{E}_D} d_{ij}\left(\dot{x}_i - \dot{x}_j\right) + \sum_{\{i,j\}\in\mathcal{E}_B} b_{ij}\left(x_i - x_j\right) = \mathrm{w}_i, \tag{3.1}$$

where m and β are respectively the intertia and local damping coefficient of each oscillator. x_i is the position of the i^{th} oscillator. w_i is an exogenous disturbance applied to the i^{th} oscillator, and b_{ij} and d_{ij} are given by $b_{ij} = \mathcal{W}_B\left(\{i,j\}\right)$, $d_{ij} = \mathcal{W}_D\left(\{i,j\}\right)$.

Based on which parameters in (3.1) are nonzero, we classify oscillator networks of the above form into three types, which are described as follows.

3.1.1 First order oscillator network

When $m = 0$ and $\mathcal{E}_D = \emptyset$, $\ddot{x}_i$ does not affect the dynamics, and so each oscillator has first order dynamics and we refer to the system as a first order oscillator network. For simplicity we assume that $\beta = 1$. In this case the following gives the dynamics of our system.

$$\dot{\mathbf{x}} = -L_B\mathbf{x} + \mathbf{w} \tag{3.2}$$

Where L_B is the weighted graph Laplacian of $\mathcal{B}$, $[\mathbf{x}] = x_i$, and $[\mathbf{w}]_i = \mathrm{w}_i$.

Remark 1. *By abuse of terminology we refer to networks of coupled subsystems* *with first order dynamics as "first order oscillator" networks although they are not oscillators in the sense that their dynamical operators have real eigenvalues.*

3.1.2 Second order oscillator network with global damping

If $m, \beta > 0$ but $\mathcal{E}_D = \emptyset$, each oscillator has second order dynamics, but the dynamics of the agents do not depend on their relative velocities. However, since $\beta > 0$, each oscillator's own velocity affects its state, we refer to this situation as global damping because the damping depends on the absolute velocity of the oscillator. In this case we obtain the following expression for the dynamics of our system.

$$\begin{bmatrix} \dot{\mathbf{x}} \\ \ddot{\mathbf{x}} \end{bmatrix} = \begin{bmatrix} 0 & I \\ -\frac{1}{m} L_B & -\frac{\beta}{m} I \end{bmatrix} \begin{bmatrix} \mathbf{x} \\ \dot{\mathbf{x}} \end{bmatrix} + \frac{1}{m} \begin{bmatrix} 0 \\ \mathbf{w} \end{bmatrix} \tag{3.3}$$

3.1.3 Second order oscillator network with local damping

If $m > 0$, $\beta = 0$, the oscillators have second order dynamics with only local damping. If we consider the special case where L_B and L_D commute, where L_D is the weighted graph Laplacian of $\mathcal{D}$, the dynamics of our system are.

$$\begin{bmatrix} \dot{\mathbf{x}} \\ \ddot{\mathbf{x}} \end{bmatrix} = \begin{bmatrix} 0 & I \\ -\frac{1}{m}L_B & -\frac{1}{m}L_D \end{bmatrix} \begin{bmatrix} \mathbf{x} \\ \dot{\mathbf{x}} \end{bmatrix} + \frac{1}{m} \begin{bmatrix} 0 \\ \mathbf{w} \end{bmatrix} \tag{3.4}$$

In the rest of this work we investigate the performance of the three types of oscillator networks described above. We show that the performance of first order oscillators networks is qualitatively very similar to that of second order oscillator networks with global damping. However, the performance of second order oscillator networks will be shown to be qualitatively different under most conditions on the structures of $\mathcal{B}$ and $\mathcal{D}$.

Chapter 4

Gramian Computation for Non-minimal Realizations

This chapter considers the problem of computing the $\mathcal{H}_2$-norm of systems for which we have a non-minimal realization. This is motivated by the fact that systems on graphs often have a zero mode due to the relative nature of the interactions between subsystems. An example of this is when the coupling is given by a weighted sum of differences between adjacent vertices. In this case, $\mathbf{u} = L_B\mathbf{x}$ where u_i is the effect of the coupling on node i, x_i is some state of the i^{th} node, and L_B is the weighted graph Laplacian of the graph describing the coupling. In this case a zero mode will appear in the dynamics of the system due to the zero eigenvalue of L_B. Chapter 3 gives several examples of such systems.

We consider some fairly subtle points concerning the observability Gramian associated with realizations of time invariant linear systems, therefore we formally state its definition here.

Definition 2. Given a pair of matrices, $A \in \mathbb{R}^{n \times n}$ and $C \in \mathbb{R}^{m \times n}$, the observability Gramian, X, of (C, A) is

$$X := \int_0^\infty e^{A^\intercal \tau} C^\intercal C e^{A\tau} d\tau \tag{4.1}$$

whenever the integral converges.

It is a standard fact that given a minimal realization, $\hat{G} = \left(\begin{array}{c|c} A & B \\ \hline C & 0 \end{array}\right)$ of a BIBO stable linear system, G, $\|G\|_{\mathcal{H}_2}^2 = \operatorname{tr}(B^\intercal X B)$ where X is observability Gramian of (C, A). In this case, X is the unique positive-definite solution to the Lyapunov equation $A^\intercal X + XA = -C^\intercal C$. Hence the $\mathcal{H}_2$-norm can be computed through purely algebraic means. We develop the framework necessary to perform similar calculations for non-minimal realizations. To do this we make use of the fact that if X exists, $\|G\|_{\mathcal{H}_2}^2 = \operatorname{tr}(B^\intercal X B)$ even when $\hat{G}$ is non-minimal. On the other hand, if A is not Hurwitz, the Lyapunov equation may not have a unique solution. [1] The following proposition extends the well known sufficient conditions for existence of the observability Gramian.

We now investigate computing the observability Gramian of certain classes of realizations that include the oscillator network models introduced in Chapter 3. We first

[1] A being Hurwitz is merely a sufficient condition for the Lyapunov equation to have a unique solution, but the state transition matrices of all the linear systems presented in Chapter 3 have a zero eigenvalue which ensures the Lyapunov equation will have multiple solutions.

present a proposition giving necessary and sufficient conditions for both the existence of the observability Gramian and a particular algebraic express for the observability Gramian to hold. We then given four Lemmas giving closed form expression for the observability Gramian and its trace in special cases which include the oscillator network models presented in Chapter 3. Part a of Proposition 1 along with Lemmas 1, 2, and 4 were previously presented in [22]. The proofs of the Lemmas given here are simplified versions.

Proposition 1. *Let $A \in \mathbb{R}^{n\times n}$, $C \in \mathbb{R}^{q\times n}$. Let $\mathscr{L} : \mathbb{R}^{n\times n} \to \mathbb{R}^{n\times n}$ be given by $\mathscr{L}(P) = A^{\intercal}P + PA$, and denote by $\varphi(\mathbf{x}_0)$ the unique solution to $\dot{\mathbf{x}} = A\mathbf{x}$ with $\mathbf{x}(0) = \mathbf{x}_0 \in \mathbb{C}^n$.*

a) The observability Gramian, X, of (C, A) exists if and only if $\forall \mathbf{x}_0 \in \mathbb{R}^n$, $C\varphi(\mathbf{x}_0) \in \mathcal{L}_2^q$.

b) Given that X exists, $X = -\mathscr{L}^{\dagger}(C^{\intercal}C)$ if and only if $\langle C\varphi(\mathbf{w}_i), C\varphi(\mathbf{w}_j)\rangle_{\mathcal{L}_2} = 0$, $\forall \mathbf{w}_i, \mathbf{w}_j \in \mathbb{C}^n$ such that (i) $\mathbf{w}_i^* A = \lambda_i(A)\mathbf{w}_i^*$, (ii) $\mathbf{w}_j^* A = \lambda_j(A)\mathbf{w}_j^*$, and (iii) $\overline{\lambda_i}(A) + \lambda_j(A) = 0$.

Proof. First we prove a). Suppose that $C\varphi(\mathbf{x}_0) \in \mathcal{L}_2^q$, $\forall \mathbf{x}_0 \in \mathbb{R}^n$. Clearly

$$C\varphi(\mathbf{e}_i), C\varphi(\mathbf{e}_j) \in \mathcal{L}_2^q, \forall 1 \le i, j \le n,$$

which implies that

$$\langle C\varphi(\mathbf{e}_i), C\varphi(\mathbf{e}_j)\rangle_{\mathcal{L}_2} = \int_0^\infty \mathbf{e}_j^\intercal e^{A^\intercal \tau} C^\intercal C e^{A\tau}\mathbf{e}_i d\tau$$

exists $\forall 1 \leq i, j \leq n$, and hence $X = \int_0^\infty e^{A^\intercal \tau} C^\intercal C e^{A\tau} d\tau$ exists. To prove the converse, note that if X exists and $\mathbf{v} \in \mathbb{R}^n$, then $\mathbf{v}^\intercal X \mathbf{v} = \int_0^\infty \varphi(\mathbf{v})^\intercal C^\intercal C \varphi(\mathbf{v}) d\tau$ converges, and hence $C\varphi(\mathbf{v}) \in \mathcal{L}_2^q$, $\forall \mathbf{v} \in \mathbb{R}^n$.

Now we prove b). Let $\lambda_1, \ldots, \lambda_n$ be the eigenvalues of A with left eigenvectors $\mathbf{w}_1, \ldots, \mathbf{w}_n$. Observe that

$$\mathscr{L} = \operatorname{span}\{\mathbf{w}_i \mathbf{w}_j^* | \overline{\lambda_i} + \lambda_j = 0\}.$$

Let $P \in \mathcal{N}(\mathscr{L})$ and write $P = \sum_{\overline{\lambda_i}+\lambda_j=0} \alpha_{ij} \mathbf{w}_i \mathbf{w}_j^*$. If we assume that

$$\langle C\varphi(\mathbf{w}_i), C\varphi(\mathbf{w}_j)\rangle_{\mathcal{L}_2} = 0, \forall \mathbf{w}_i, \mathbf{w}_j \in \mathbb{C}^n \tag{4.2}$$

such that $\mathbf{w}_i^* A = \lambda_i(A)\mathbf{w}_i^*$, $\mathbf{w}_j^* A = \lambda_j(A)\mathbf{w}_j^*$, and $\overline{\lambda_i}(A) + \lambda_j(A) = 0$, we get that

$$\begin{aligned}
\langle P, X\rangle_F &= \operatorname{tr}\left(\int_0^\infty e^{A^\intercal \tau} C^\intercal C e^{A\tau} d\tau \sum_{\overline{\lambda_i}+\lambda_j=0} \alpha_{ij} \mathbf{w}_i \mathbf{w}_j^*\right) \\
&= \sum_{\overline{\lambda_i}+\lambda_j=0} \alpha_{ij} \int_0^\infty \mathbf{w}_j^* e^{A^\intercal \tau} C^\intercal C e^{A\tau} \mathbf{w}_i d\tau \\
&= \sum_{\overline{\lambda_i}+\lambda_j=0} \alpha_{ij} \langle C\varphi(\mathbf{w}_i), C\varphi(\mathbf{w}_j)\rangle_{\mathcal{L}_2} = 0.
\end{aligned}$$

Therefore X is orthogonal to $\mathscr{N}(\mathscr{L})$. It is easy to verify that $\mathscr{L}(X) = -C^{\intercal}C$ [2], and therefore $X = -\mathscr{L}^{\dagger}(C^{\intercal}C)$.

To show the converse, suppose $\exists \mathbf{w}_i, \mathbf{w}_j$ such that $\overline{\lambda_i} + \lambda_j = 0$ and

$$\langle C\varphi(\mathbf{w}_i), C\varphi(\mathbf{w}_j)\rangle_{\mathcal{L}_2} \neq 0. \tag{4.3}$$

Then $\left\langle X, \mathbf{w}_i\mathbf{w}_j^*\right\rangle_F = \langle C\varphi(\mathbf{w}_i), C\varphi(\mathbf{w}_j)\rangle_{\mathcal{L}_2} \neq 0$ and hence $X \notin (\mathscr{N}(\mathscr{L}))^{\perp}$. Since X satisfies $\mathscr{L}(X) = -C^{\intercal}C$, $-\mathscr{L}^{\dagger}(C^{\intercal}C) \in (\mathscr{N}(\mathscr{L}))^{\perp}$. Hence $X \neq -\mathscr{L}^{\dagger}(C^{\intercal}C)$. $\square$

The conditions for the existence of X given in Proposition 1 can be simplified under a restriction on A. This is formalized in the following Proposition.

Proposition 2. *If all the unstable modes of $A \in \mathbb{R}^{n\times n}$ are non-defective, then $C\varphi(\mathbf{x}_0) \in \mathcal{L}_2^q$, $\forall \mathbf{x}_0 \in \mathbb{R}^n$ is equivalent to the following. If $\mathrm{Re}(\lambda_i(A)) \geq 0$, then $\forall \mathbf{v} \in \mathbb{C}^n$ such that $A\mathbf{v} = \lambda_i(A)\mathbf{v}$, $C\mathbf{v} = 0$.*

Proposition 1 gives conditions for the existance of the observability Gramian. The following lemmas give closed form expressions for X and commonly used functions thereof for special cases that correspond to commonly studied systems distributed over graphs. Lemmas 1 and 2 are useful for computing the $\mathcal{H}_2$-norm of a system composed of first order subsystems distributed over a graph, e.g. a first order oscillator network. In the proofs of Lemmas 1 and 2 we compute X or its trace directly from (4.1). However, the proofs of Lemmas 3 and 4 use the method of solving the Lyapunov

[2] T. Kailath [23] gives the well known proof that X satisfies $\mathscr{L}(X) = -C^{\intercal}C$ when A is Hurwitz. The same proof will hold as long as X exists.

equation while imposing additional conditions that ensure the solution that is found is in fact the observability Gramian.

Lemma 1. *Let $A \in \mathbb{R}^{n\times n}$ and $C \in \mathbb{R}^{q\times n}$ such that $A \leq 0$ and $\mathcal{N}(A) \subseteq \mathcal{N}(C)$. If A and $C^\intercal C$ commute, then the observability Gramian, X, of (C, A) exists and is given by $X = -\frac{1}{2}A^\dagger C^\intercal C$.*

Proof. Because A is symmetric, it is non-defective. Therefore by Proposition 2, $A \leq 0$ and $\mathcal{N}(A) \subseteq \mathcal{N}(C)$ ensure that X exists by part a) of Proposition 1. Therefore we have

$$X = \int_0^\infty e^{A^\intercal\tau} C^\intercal C e^{A\tau} d\tau = \int_0^\infty C^\intercal C e^{2A\tau} d\tau. \tag{4.4}$$

From the properties of the Moore-Penrose pseudoinverse, we know that[3]

$$A^\dagger A = I - \sum_{\lambda_i(A)=0} \mathbf{w}_i \mathbf{w}_i^*.$$

$\mathcal{N}(A) \subseteq \mathcal{N}(C)$ ensures that $C\mathbf{w}_i = 0, \forall A\mathbf{w}_i = 0$. Therefore $\frac{d}{dt}\left(\frac{1}{2}C^\intercal C A^\dagger e^{2At}\right) = C^\intercal C A^\dagger A e^{2At} = C^\intercal C e^{2At}$. We can therefore conclude from (4.4) that $X = -\frac{1}{2}A^\dagger C^\intercal C$.

□

The following lemma is a generalization of a result given by Siami and Motee [11].

Lemma 2. *Let $A \in \mathbb{R}^{n\times n}$ and $C \in \mathbb{R}^{q\times n}$ such that $A \leq 0$ and $\mathcal{N}(A) \subseteq \mathcal{N}(C)$. The observability Gramian, X, of (C, A) exists and its trace is given by* $\mathrm{tr}(X) =$

[3]Since A is symmetric, $\exists U = [\mathbf{w}_1 \cdots \mathbf{w}_n]$ orthogonal such that $U^\intercal AU = D$ where $D = \mathrm{diag}\, \lambda_1, \ldots, \lambda_n$. Therefore $A^\dagger A = Q^\intercal D^\dagger DQ = \sum_{\lambda_i \neq 0} \mathbf{w}_i\mathbf{w}_i^* = I - \sum_{\lambda_i=0} \mathbf{w}_i\mathbf{w}_i^*$.

$-\frac{1}{2}\mathrm{tr}\left(A^{\dagger}C^{\intercal}C\right)$.

Proof. As in the case of Lemma 1, Propositions 1 and 2 show that the observability Gramian, X, of (C, A) exists. Therefore

$$\mathrm{tr}\left(X\right) = \mathrm{tr}\left(\int_0^{\infty} e^{A^{\intercal}\tau}C^{\intercal}Ce^{A\tau}d\tau\right) = \int_0^{\infty} \mathrm{tr}\left(C^{\intercal}Ce^{2A\tau}\right)d\tau.$$

By the same argument used in the proof of Lemma 1, we have $\mathrm{tr}\left(X\right) = -\frac{1}{2}\mathrm{tr}\left(A^{\dagger}C^{\intercal}C\right)$.

□

The following Lemmas give similar results to Lemmas 1 and 2 for realizations with state transition matrices of the form $A = \begin{bmatrix} 0 & I \\ F & G \end{bmatrix}$ where F and G are symmetric, instead of A itself being symmetric. These results are useful for evaluating the $\mathcal{H}_2$-norm of a network of second order systems.

Lemma 3. *Let* $A \in \mathbb{R}^{2n\times 2n}$ *and* $C \in \mathbb{R}^{q\times 2n}$ *be partitioned as* $A = \begin{bmatrix} 0 & I \\ F & G \end{bmatrix}$ *and* $C = \begin{bmatrix} H & 0 \end{bmatrix}$, *where* $0 \geq F, G \in \mathbb{R}^{n\times n}$ *and* $H \in \mathbb{R}^{q\times n}$ *are such that* F, G, *and* $H^{\intercal}H$ *commute pairwise, and* $\mathcal{N}\left(F\right) \cup \mathcal{N}\left(G\right) \subseteq \mathcal{N}\left(H\right)$. *Partition the observability Gramian,* X, *as* $X = \begin{bmatrix} X_{11} & X_{12} \\ X_{12}^{\intercal} & X_{22} \end{bmatrix}$. *Under these conditions* $X_{22} = \frac{1}{2}G^{\dagger}F^{\dagger}H^{\intercal}H$.

Proof. We will first show that (C, A) satisfies the conditions of Proposition 1. Let $\mathbf{w}_1, \ldots, \mathbf{w}_n$ be the orthonormal eigenvectors of F and G. Let

$$S_i = \mathrm{span}\left\{ \begin{bmatrix} \mathbf{w}_i \\ 0 \end{bmatrix}, \begin{bmatrix} 0 \\ \mathbf{w}_i \end{bmatrix} \right\}.$$

Let $\mathbf{x}_0 \in \mathbb{R}^{2n}$. There exist $\mathbf{x}_i \in S_i$ such that $\mathbf{x}_0 = \sum_{i=1}^{n} \mathbf{x}_i$. S_i is A invariant, so

$$C\varphi\left(\mathbf{x}_0, t\right) = \sum_{i=1}^{n} C\varphi_i\left(\mathbf{x}_i, t\right)$$

where $\varphi_i\left(\mathbf{x}_i, t\right) \in S_i$, $\forall 1 \leq i \leq n$.

We show that $C\varphi_i\left(\mathbf{x}_i, t\right) \in \mathcal{L}_2^q$, and hence $C\varphi\left(\mathbf{x}_0, t\right) \in \mathcal{L}_2^q$. Observe that if we take $\mathcal{B}_i = \left\{ \begin{bmatrix} \mathbf{w}_i \\ 0 \end{bmatrix}, \begin{bmatrix} 0 \\ \mathbf{w}_i \end{bmatrix} \right\}$ as our basis for S_i,

$$\left[\varphi_i\left(\mathbf{x}_i, t\right)\right]_{\mathcal{B}_i} = e^{A_i t}\left[\mathbf{x}_i\right]_{\mathcal{B}_i}$$

where $A_i = \begin{bmatrix} 0 & 1 \\ \lambda_i\left(F\right) & \lambda_i\left(G\right) \end{bmatrix}$. Here $\left[\mathbf{x}_i\right]_{\mathcal{B}_i}$ denotes the representation of $\mathbf{x}_i$ in $\mathcal{B}_i$. A_i is Hurwitz unless $\lambda_i\left(F\right) = 0$ or $\lambda_i\left(G\right) = 0$. Since $\mathcal{N}\left(F\right) \cup \mathcal{N}\left(G\right) \subseteq \mathcal{N}\left(H\right)$, if A_i is not Hurwitz, then $CS_i = \{0\}$. Therefore

$$C\varphi\left(\mathbf{x}_0, t\right) \in \mathcal{L}_2^q,\ \forall \mathbf{x}_0 \in \mathbb{R}^{2n},$$

and hence Proposition 1 tells us that X exists.

X satisfies[4] $\mathscr{L}\left(X\right) = -C^{\intercal}C$ where $\mathscr{L} : \mathbb{R}^{2n\times 2n} \to \mathbb{R}^{2n\times 2n}$ is given by $\mathscr{L}\left(P\right) =$

[4]T. Kailath [23] gives the well known proof that X satisfies $\mathscr{L}\left(X\right) = -C^{\intercal}C$ when A is Hurwitz. The same proof will hold as long as X exists.

$A^\intercal P + PA$. Writing this out block-wise yields

$$FX_{12}^\intercal + X_{12}F = -H^\intercal H, \tag{4.5a}$$

$$GX_{22} + X_{22}G = -X_{12} - X_{12}^\intercal. \tag{4.5b}$$

It can be shown using the definition of the observability Gramian that X_{12} commutes with F and G. Therefore, from (4.5a) we get that

$$G^\dagger F^\dagger F\left(X_{12}^\intercal + X_{12}\right) = -G^\dagger F^\dagger H^\intercal H.$$

Since $XS_i = \{0\}\,, \forall S_i \subseteq \mathcal{N}(H)$, we can use an argument similar to that made in the proof of Lemma 1 to show that

$$F^\dagger F\left(X_{12}^\intercal + X_{12}\right) = \left(X_{12}^\intercal + X_{12}\right),$$

hence

$$G^\dagger\left(X_{12}^\intercal + X_{12}\right) = -G^\dagger F^\dagger H^\intercal H.$$

Since X_{22} also commutes with F and G, from (4.5b) we have that $2G^\dagger G X_{22} = -G^\dagger\left(X_{12}^\intercal + X_{12}\right)$, and using the same argument as for (4.5a), we have that $X_{22} = -G^\dagger\left(X_{12}^\intercal + X_{12}\right)$. Therefore

$$X_{22} = \frac{1}{2}G^\dagger F^\dagger H^\intercal H,$$

which concludes our proof. $\square$

Lemma 4. *Let $A \in \mathbb{R}^{2n\times 2n}$ and $C \in \mathbb{R}^{q\times 2n}$ be partitioned as $A = \begin{bmatrix} 0 & I \\ F & G \end{bmatrix}$ and $C = \begin{bmatrix} H & 0 \end{bmatrix}$, where $0 \geq F, G \in \mathbb{R}^{n\times n}$ and $H \in \mathbb{R}^{q\times n}$ are such that F and G commute, and $\mathcal{N}(F) \cup \mathcal{N}(G) \subseteq \mathcal{N}(H)$. Partition the observability Gramian, X, as $X = \begin{bmatrix} X_{11} & X_{12} \\ X_{12}^{\intercal} & X_{22} \end{bmatrix}$. Under these conditions $\operatorname{tr}(X_{22}) = \frac{1}{2}\operatorname{tr}\left(G^{\dagger}F^{\dagger}H^{\intercal}H\right)$.*

Proof. As in the case of Lemma 3, part a) of Proposition 1 is satisfied and $\mathscr{L}(X) = -C^{\intercal}C$. Denote by $\mathbb{S}^{n\times n}$ the set of $n \times n$ real symmetric matrices. Since the set of matrices in $\mathbb{S}^{n\times n}$ that commute with F is a linear subspace of $\mathbb{S}^{n\times n}$, there exist matrices $Q_1, Q_2 \in \mathbb{S}^{n\times n}$ such that $Q_1 + Q_2 = H^{\intercal}H$ where Q_1 commutes with F and $\langle Q_2, P\rangle_F = 0$, $\forall FP = PF$. One can show that the trace of the $(2,2)$ block of $\int_0^\infty e^{A^{\intercal}\tau} \begin{bmatrix} Q_2 & 0 \\ 0 & 0 \end{bmatrix} e^{A\tau} d\tau$ is zero. Therefore,

$$\operatorname{tr}(X_{22}) = \operatorname{tr}\left(\begin{bmatrix} 0 & I \end{bmatrix} \int_0^\infty e^{A^{\intercal}\tau} \begin{bmatrix} Q_1 & 0 \\ 0 & 0 \end{bmatrix} e^{A\tau} d\tau \begin{bmatrix} 0 \\ I \end{bmatrix}\right).$$

It then follows from Lemma 3 that $\operatorname{tr}(X_{22}) = \frac{1}{2}\operatorname{tr}\left(G^{\dagger}F^{\dagger}Q_1\right)$. Additionally, since $F^{\dagger}G^{\dagger}$ commutes with F, $\operatorname{tr}\left(F^{\dagger}G^{\dagger}Q_2\right) = 0$. Therefore $\operatorname{tr}(X_{22}) = \frac{1}{2}\operatorname{tr}\left(G^{\dagger}F^{\dagger}H^{\intercal}H\right)$. $\square$

Chapter 5

Performance Measures for Oscillator Networks with Local and Global Damping

In this chapter we examine the performance of linear oscillator networks. We consider first order oscillator networks of the form (3.2), second order oscillator networks with global damping of the form (3.3), and seconder order oscillator networks with local damping of the form (3.4). We apply the results of Chapter 4 to these system models. We first consider applying a disturbance to a single oscillator in the network and examining the value of certain specific performance measures of interest. We then consider applying disturbances to all the oscillators in the network and show how to compute a large class of performance measures. In both cases we connect the performance of the oscillator network to the concept of effective resistance. To make these results concrete we apply them to special graph structures where we have analytical expressions for the effective resistance.

Additionally, we consider a special case a of computing the effective resistance between two vertices in a weighted graph. Specifically, we give a formula for the effective resistance between two vertices in a graph where there is only one path between the two vertices in question. While the result itself is intuitive from a circuit theory point of view, we provide a graph theoretic proof of the result that requires only the definition of effective resistance as presented in Chapter 2, and does not require Kirchoff's circuit laws or Ohm's law.

5.1 Performance with Localized Disturbances

We now investigate the effects of applying a stochastic disturbance to one oscillator in the network, and measure how the network's sensitivity to disturbances varies with location. Additionally, we present a bound on the network performance when some number, $k < n$, of oscillators have exogenous disturbances applied to them. This bound is in terms of the spectral properties of the graphs underlying the oscillator network, and shows how the results of Chapter 4 are related to previous works [11, 20, 24].

Definition 3. Consider an oscillator network given by (3.2), (3.3), or (3.4). The input localized performance of the oscillator network, $P^i_{L_G}$, is given by

$$P^i_{L_G} := \lim_{t\to\infty} E\left[\mathbf{x}^\intercal L_G \mathbf{x}\right]. \tag{5.1}$$

Here $\mathbf{x}$ is given by (3.2), (3.3), or (3.4) where $\mathrm{w}_j = 0$, $\forall j \neq i$, and w_i is unit strength white Gaussian noise.

Remark 2. *consider the BIBO stable system, G, with realization $\hat{G} = \left(\begin{array}{c|c} A & \mathbf{e}_i \\ \hline C & 0 \end{array}\right)$ where $n+1 \leq i \leq 2n$, A is the state transition matrix from* (3.2), (3.3), *or* (3.4), *and $C = L_G^{\frac{1}{2}}$ for a first order oscillator network or $C = \begin{bmatrix} L_G^{\frac{1}{2}} & 0 \end{bmatrix}$ for a second order oscillator network. Under these conditions, $P^i_{L_G} = \|G\|^2_{\mathcal{H}_2}$.*

We now use remark 2 to derive expressions for $P^i_{L_G}$ for two special forms of L_G. The first form we consider is $L_G = I - \frac{1}{2}n$. In this case, $L_G^{\frac{1}{2}} = L_G$ and so $\mathbf{y} = L_G^{\frac{1}{2}}\mathbf{x}$ is the vector of deviations of x_i from $\operatorname{mean}(\mathbf{x})$. Therefore, $P^i_{L_G}$ is the steady state variance of $\mathbf{x}$. The second form we consider is $L_G = \alpha L_B$, $\alpha \in \mathbb{R}$. In this case, $P^i_{L_G}$ measures the interactions between oscillators during resynchronization.

Remark 3. *In this work we consider $L_G = I - \frac{1}{n}J$ because then $P^i_{L_G}$ measures the coherence of the network. However, analogous results can be derived for $L_G = \frac{1}{n}I - J$, in which case $\mathbf{x}^\intercal L_G \mathbf{x}$ corresponds to the total short range disorder in the network. The total short range disorder is often studied in the context of consensus networks.*

Theorem 1. *Consider a first order oscillator network given by* (3.2) *or a second order oscillator network with global damping given by* (3.3)*. The following table gives* *the values of* $P^i_{L_G}$ *for* $L_G = I - \frac{1}{n}J$ *and* $L_G = \alpha L_B$.

Net. Type	$L_G = I - \frac{1}{n}J$	$L_G = \alpha L_B$
F. O.	$\frac{1}{2n}\left(\sum_{k=1}^{n} R_{Bik} - \frac{1}{n}R_{Btot}\right)$	$\frac{\alpha}{2}\left(1 - \frac{1}{n}\right)$
S. O.(G.D.)	$\frac{1}{2n\beta}\left(\sum_{k=1}^{n} R_{Bik} - \frac{1}{n}R_{Btot}\right)$	$\frac{\alpha}{2\beta}\left(1 - \frac{1}{n}\right)$

Proof. The observability Gramian for first order networks can be found using Lemma 1 with $C = I - \frac{1}{n}J$ and $C = (\alpha L_B)^{\frac{1}{2}}$. Similarly, the observability Gramian for second order networks with global damping follow from Lemma 3 with $H = I - \frac{1}{n}J$ and $H = (\alpha L_B)^{\frac{1}{2}}$. The results for $L_G = I - \frac{1}{n}J$ then follow from the fact that if L is the weighted graph Laplacian of graph $\mathcal{G}$, then [25]

$$L^{\dagger} = -\frac{1}{2}\left(R - \frac{1}{n}(RJ + JR) + \frac{1}{n^2}JRJ\right). \tag{5.2}$$

□

Theorem 1 tells us that for oscillator networks that are first order or second order with global damping, the effects of a single disturbance do not depend on where in the network the disturbance is applied when $L_G = \alpha L_B$. This will not be true for general L_G, e.g. in the case $L_G = I - \frac{1}{n}J$, the performance will vary with the disturbance location.

Theorem 1 tells us that when $L_G = \alpha L_B$ the effects of a single disturbance on a first order oscillator networks and second order oscillator networks with global damping do not depend on where in the network the disturbance is applied. This will not be true for general L_G, e.g. in the case $L_G = I - \frac{1}{n}J$, the performance will vary with the disturbance location.

Theorem 2. *Consider a second oscillator network with local damping given by* (3.4)*. If* $L_G = \alpha L_B$*,*

$$P^i_{L_G} = \frac{\alpha}{2}\left(\frac{1}{n}\sum_{k=1}^{n} R_{Dik} - \frac{1}{n^2}R_{Dtot}\right).$$

Proof. The theorem follows from Lemma 3 and (5.2), which was used in the proof of Theorem 1. □

Remark 4. *The result analogous to Theorem 2 for* $L_G = \alpha L_D$ *is*

$$P^i_{L_G} = \frac{1}{2}\left(\frac{1}{n}\sum_{k=1}^{n} R_{Bik} - \frac{1}{n^2}R_{Btot}\right).$$

The result holds because $L_B^{\dagger}$ *and* $L_D^{\dagger}$ *commute.*

Theorem 2 gives results analogous to Theorem 1, but for oscillator networks with local damping. We now present a result that is applicable when there are disturbances applied at multiple oscillators in a network.

Theorem 3. *Consider an oscillator network given by* (3.3)*. Partition the nodes into* $\mathcal{V} = \mathcal{V}_1 \cup \mathcal{V}_2$ *with* $k = |\mathcal{V}_1|$*. Let* $\mathrm{w}_i = 0, \forall i \in \mathcal{V}_2$ *and* w_j *be independent, unit strength, Gaussian white noise* $\forall j \in \mathcal{V}_1$*. If* L_G *and* L_B *commute, then*

$$\lim_{t\to\infty} E\left[\mathbf{x}^{\intercal} L_G \mathbf{x}\right] \leq \frac{1}{2\beta}\sum_{i=1}^{k}\left(\frac{\lambda_i\left(L_G\right)}{\lambda_i\left(L_B\right)}\right)^{\downarrow}.$$

Here $\left(\frac{\lambda_i(L_G)}{\lambda_i(L_B)}\right)^{\downarrow}$ *denotes the non-increasing ordering of* $\operatorname{diag}\left(\Sigma_B^{\dagger}\Sigma_G\right)$*, where* $L_B = Q^{\intercal}\Sigma_B Q$ *and* $Q^{\intercal}\Sigma_G Q$ *for some real orthogonal* $Q \in \mathbb{R}^{n\times n}$*.*

Remark 5. *The same result (without the* β *term) holds for oscillator networks of the form* (3.2)*.*

Proof. The theorem follows from Lemma 3 and the fact that the eigenvalues of a Hermitian matrix majorize its diagonal elements. □

Theorem 3 gives an expression for the performance of an oscillator network when disturbances are applied at multiple nodes. This result is conceptually similar to many prior works on oscillator network performance in that the expression involves the spectral properties of the graphs underlying the oscillator network. See e.g. [10], [11], and [21].

5.2 Performance with Distributed Disturbances

In this section we present the main results of this work, which connects the concept of effective resistance to the performance of oscillator networks. We begin by stating three simple results that follow immediately from the results presented in Chapter 4. We then obtain results for the nodal performance, P_{ij}, which we define, of the network with respect to an arbitrary pair of nodes for the three types of oscillator networks presented in Section 3. Finally we show how P_{ij} can be used to compute a large class of performance measures for oscillator networks.

The following consequence of the results of Chapter 4 gives algebraic expressions for the $\mathcal{H}_2$-norms of oscillator networks. While the expressions given in this theorem are not especially useful on their own, they provide an intermediate step between the abstract results of Chapter 4 and the results given later in this chapter.

Theorem 4. *Consider a first order oscillator network of the form* (3.2)*, a second order oscillator network with global damping of the form* (3.3)*, or a second order oscillator network of the form* (3.4)*. If we define the system G as being from the input $\mathbf{w}$ to the output $\mathbf{y} = L_G^{\frac{1}{2}}$ where L_G is a weighted graph Laplacian, then the following expressions for $\|G\|_{\mathcal{H}_2}^2$ hold.*

First order oscillator network

$$\|G\|_{\mathcal{H}_2}^2 = \frac{1}{2}\mathrm{tr}\left(L_B^{\dagger} L_G\right) \tag{5.3}$$

Second order oscillator network with global damping

$$\|G\|_{\mathcal{H}_2}^2 = \frac{1}{2\beta}\mathrm{tr}\left(L_B^{\dagger} L_G\right) \tag{5.4}$$

Second order oscillator network with local damping

$$\|G\|_{\mathcal{H}_2}^2 = \frac{1}{2}\mathrm{tr}\left(L_D^\dagger L_B^\dagger L_G\right) \tag{5.5}$$

Proof. The kernel of any weighted graph Laplacian that is associated with a connected graph is span $\mathbf{1}$, and hence $\mathcal{N}\, L_B \cup \mathcal{N}\, L_D \subseteq \mathcal{N}\, L_G$. Additionally, $L_B, L_D \geq 0$ and hence the conditions of Lemmas 2 and 4 are satisfied. □

The parts of Theorem 4 pertaining to first order oscillator networks and second order oscillator networks with global damping were previously reported in [11] and [20] respectively.

We now move on to the main results of this work, which consider the nodal performance of two nodes in an oscillator network.

Definition 4. Consider an oscillator network of the form (3.2), (3.3), or (3.4) where $\mathbf{w}(t)$ is a Gaussian white noise vector with each element having unit strength. The nodal performance, denoted by P_{ij}, of the pair of oscillators $\{i, j\}$ is the steady state expectation of the squared difference between x_i and x_j. i.e.

$$P_{ij} := \lim_{t\to\infty} E\left[(x_i - x_j)^2\right]. \tag{5.6}$$

Remark 6. *It is true that* $P_{ij} = \|G\|_{\mathcal{H}_2}^2$*, where* G *is the system with input to state dynamics given by* (3.2)*,* (3.3)*, or* (3.4) *and output* $y = (\mathbf{e}_i - \mathbf{e}_j)^\intercal \mathbf{x}$*. Therefore, as* *long as the observability Gramian of* (C, A) *exists, we have that* $P_{ij} = \operatorname{tr}(B^{\intercal} X B)$ *where* X *is the observability Gramian of* (C, A).

The nodal performance of pair $\{i, j\}$ has several interpretations. If $\{i, j\} \in \mathcal{E}_B$, then P_{ij} quantifies how much the edge $\{i, j\}$ is used to maintain synchrony. If $\{i, j\}$ is instead chosen so that i and j are far apart in the network, P_{ij} quantifies the coherence of the subnetwork connecting i and j in terms of long range disorder [15]. By the subnetwork connecting i and j we mean the network that consists of all oscillators and edges on all the paths between i and j. More generally, $\{i, j\}$

Theorem 5. *Given an oscillator network with dynamics given by* (3.2)*, the nodal performance of* $\{i, j\}$ *is given by*

$$P_{ij} = \frac{1}{2} R_{Bij},$$

where R_{Bij} *is the effective resistance between* i *and* j *in* $\mathcal{B}$ *and given an oscillator network with dynamics given by* (3.3)*, the nodal performance of* $\{i, j\}$ *is given by*

$$P_{ij} = \frac{1}{2\beta} R_{Bij}.$$

Proof. The result follows immediately from Lemmas 2 and 4 along with the definition of R_{Bij}. $\square$

Theorem 5 gives us closed form expressions for P_{ij} in the cases of first order oscillator networks and second order oscillator networks with global damping. We next consider the case of second order oscillator networks with local damping, and derive upper and lower bounds on P_{ij}, which are given in the following two theorems.

Theorem 6. *Consider a second order oscillator network with local damping whose dynamics are given by* (3.4) *where L_B and L_D commute. In this case,*

$$P_{ij} \leq \frac{1}{2} n R_{Bij} R_{Dij}$$

Here R_{Bij} and R_{Dij} are the effective resistances between i and j in $\mathcal{B}$ and $\mathcal{D}$ respectively.

Proof. Let $\mathbf{v} = \mathbf{e}_i - \mathbf{e}_j$. Use Lemma 4 to obtain that $P_{ij} = \frac{1}{2} \left\langle L_B^\dagger \mathbf{v}, L_D^\dagger \mathbf{v} \right\rangle$, and then use the Cauchy-Schwarz inequality to get

$$P_{ij} \leq \frac{1}{2} \sqrt{\left\langle L_B^\dagger \mathbf{v}, L_B^\dagger \mathbf{v} \right\rangle \left\langle L_D^\dagger \mathbf{v}, L_D^\dagger \mathbf{v} \right\rangle}. \tag{5.7}$$

It is true that if L is the weighted graph Laplacian of graph $\mathcal{G}$, then [25]

$$L^\dagger = -\frac{1}{2} \left(R - \frac{1}{n} (RJ + JR) + \frac{1}{n^2} JRJ \right) \tag{5.8}$$

Here $R = [R_{ij}]$ is the matrix of effective resistances in graph $\mathcal{G}$. It is easy to show using this fact that

$$\left\langle L_B^\dagger \mathbf{v}, L_B^\dagger \mathbf{v} \right\rangle \leq nR_{Bij}^2,$$
$$\left\langle L_D^\dagger \mathbf{v}, L_D^\dagger \mathbf{v} \right\rangle \leq nR_{Dij}^2.$$

It is then clear from (5.7) that $P_{ij} \leq nR_{Bij}R_{Dij}$. □

Theorem 7. *Consider a second order oscillator network with local damping whose dynamics are given by* (3.4) *where* $L_D = \gamma L_B,\ \gamma > 0$. *In this special case we have the following lower bound.*

$$\frac{1}{4\gamma} R_{Bij}^2 \leq P_{ij}.$$

Proof. This lower bound follows from the fact that if $M_1, M_2 \in \mathbb{R}^{n \times n}$ are symmetric, then $\operatorname{tr}(M_1^2 M_2^2) \geq \operatorname{tr}\left((M_1 M_2)^2\right)$ [26]. □

One special case where L_B and L_D commute is when either $\mathcal{B}$ or $\mathcal{D}$ is complete with uniform edge weights. E. Sjödin [24] showed this for complete $\mathcal{B}$ with uniform edge weights and $\mathcal{D}$ with uniform edge weights. Because the weighted graph Laplacian, L_B, of a complete graph with uniform edge weights has only two eigenspaces, span $\mathbf{1}$ and $(\operatorname{span} \mathbf{1})^\perp$, any other weighted graph Laplacian will commute with L_B. We now give a closed form expression for P_{ij} in this case, which corresponds to a network of oscillators where each oscillator is damped relative of the average velocity of all the other oscillators in the network.

Theorem 8. *Consider a second order oscillator network with local damping whose dynamics are given by* (3.4) *where* $L_D = \beta\left(I - \frac{1}{n}J\right)$, $\beta > 0$. *In this case* $P_{ij} = \frac{1}{2\beta}R_{Bij}$.

Proof. By the the preceding discussion, L_D will commute with any weighted graph Laplacian, so we can use Lemma 4 and the fact that $\left(I - \frac{1}{n}J\right)^{\dagger} = I - \frac{1}{n}J$ to show that $P_{ij} = \frac{1}{2\beta}\mathrm{tr}\left(\mathbf{v}^{\intercal}\left(I - \frac{1}{n}J\right)L_B^{\dagger}\mathbf{v}\right) = \frac{1}{2\beta}R_{Bij}$. Here $\mathbf{v} = \mathbf{e}_i - \mathbf{e}_j$. $\square$

Theorem 8 tells us that when each oscillator is locally damped to every other oscillator in the network with uniform damping constant $\frac{\beta}{n}$, the nodal performance in the network is the same as the case of global damping. This is because $\beta\left(I - \frac{1}{n}J\right)$ and βI commute and have identical eigenvalues except for the one associated with the eigenvector $\mathbf{1}$. This eigenvector corresponds to the average motion of the oscillators which is not observable through our chosen output.

To compare the nodal performance of second order oscillator networks with local and global damping, consider two second order oscillator networks: one with global damping and dynamics given by (3.3) and one with local damping and dynamics given by (3.4). $\mathcal{B}$ is the same for both networks. If $L_D = \beta\left(I - \frac{1}{n}J\right)$, then Theorems 5 and 8 tell us that the nodal performance is the same for the two networks. On the other hand, if $L_D = \gamma L_B$, Theorem 7 tells us that the nodal performance is worse for the local damping network when R_{Bij} is sufficiently large. Therefore in general the nodal performance of oscillator networks with local damping may or may not be worse than the nodal performance of the corresponding network with global damping.

Now we show how to construct a large class of performance measures that quantify the performance of oscillator networks with distributed disturbances. Consider the performance measure for an oscillator network

$$P_{L_G} := \lim_{t \to \infty} E\left[\mathbf{x}^\intercal L_G \mathbf{x}\right] \tag{5.9}$$

where L_G is the weighted graph Laplacian of some arbitrary graph with vertex set $\mathcal{V}$, $\mathcal{G} = (\mathcal{V}, \mathcal{E}_G, \mathcal{W}_G)$. The results from this section can be applied to performance measures of this form by writing $\mathbf{x}^\intercal L_G \mathbf{x} = \sum_{\{i,j\} \in \mathcal{E}_G} g_{ij} \left(x_i - x_j\right)^2$, where $\mathcal{E}_G$ is the edge set of $\mathcal{G}$ and $g_{ij} = \mathcal{W}_G\left(\{i,j\}\right)$ is weight of each edge. Therefore,

$$P_{L_G} = \sum_{\{i,j\} \in \mathcal{E}_G} g_{ij} P_{ij}.$$

Therefore, Theorems 5, 6, and 7 can be used to obtain results for performance measures of the form (5.9).

Remark 7. *Let $l, k \in \mathcal{V}$. If $\mathcal{E}_G = \{\{l,k\}\}$ (i.e. the only edge in the graph is the one connecting l and k) and $g_{lk} = 1$, then $P_{L_G} = P_{ij}$.*

5.2.1 Illustrative examples: specific graph structures

In order to illustrate the results of Section 5.2 as well as compare our effective resistance based results to previous work, we now consider oscillator networks distributed over graphs with specific structures. We first examine the case of a d-dimensional lattice, and apply the results of Section 5.2 to obtain asymptotic bounds on the coherence of oscillator networks on lattices with local and global damping. We then look at line graphs and obtain exact results for the coherence of subsections of the network. Finally, we examine oscillator networks distributed over complete graphs and see that the effective resistance based results in Section 5.2 provide an explanation for why oscillator networks on more connected graphs are more coherent.

Example (d-dimensional lattice)**.** Consider a homogeneous oscillator network with n oscillators distributed over a d-dimensional hypercubic lattice ($\mathcal{B}$ and $\mathcal{D}$ are d-dimensional lattices). For simplicity we assume that $\mathcal{B}$ and $\mathcal{D}$ have edge weights that are uniformly one. For $d \geq 2$ we assume that the lattice is a hypercube. The greatest effective resistance between any two vertices in the network is that between vertices in opposite corners, which is given by

$$R_{max} = \begin{cases} n-1 & : d = 1 \\ 2\dfrac{\left(\dfrac{1}{d}\right)^{n^{1/d}-1} - 1}{1-d} & : d \geq 2 \end{cases}. \tag{5.10}$$

Network Type	$\lim_{n\to\infty} P_{ij}$
First Order	$\lim_{n\to\infty} P_{ij} = \begin{cases} \frac{1}{2}(n-1) & : d=1 \\ \frac{1}{d-1} & : d \geq 2 \end{cases}$
S.O. w/ global damping	$\lim_{n\to\infty} P_{ij} = \begin{cases} \frac{1}{2\beta}(n-1) & : d=1 \\ \frac{1}{\beta(d-1)} & : d \geq 2 \end{cases}$
S.O. w/ local damping	$\left.\begin{matrix} \frac{1}{2\gamma}(n-1)^2 : d=1 \\ \frac{1}{\gamma(d-1)^2} \quad : d \geq 2 \end{matrix}\right\} \leq \lim_{n\to\infty} P_{ij} \leq \begin{cases} \frac{n}{2\gamma}(n-1)^2 : d=1 \\ \frac{n}{\gamma(d-1)^2} \quad : d \geq 2 \end{cases}$

Table 5.1: Asymptotic bounds on $P_{ij} = \lim_{t\to\infty} E\left[(x_i - x_j)^2\right]$ for three types of oscillator networks distributed over a hypercubic lattice. i and j are assumed to be in opposite corners of the lattice.

The coherence of the network in terms of long range disorder is measured by P_{ij} where i and j are in opposite corners of the lattice. Using the results of Section 5.2 and the above expression for R_{max}, we can compute asymptotic results for P_{ij}. Table 5.1 gives these results.

Bamieh et. al. [15] used Fourier analysis to obtain upper bounds on the coherence of second order subsystems distributed over d-dimensional tori with local and absolute velocity feedback. The order with which their upper bound depends on n decreases for $1 \leq d \leq 5$. Our upper bound is comparable for $d = 1$ and 2, but the order of our bound in n is constant for $d \geq 2$. However, the effective resistance based bounds presented here have the advantage to being applicable to systems distributed over arbitrary graphs, whereas the Fourier analysis method is limited to graphs with the structure of a locally compact Abelian group.

Remark 8. *The results derived here are for oscillator networks on lattice graphs. It is reasonable to compare these results to those derived for toroidal graphs because if* $R^L_{max}(n)$ *is the effective resistance between opposite corners in a d-dimensional lattice graph with* n *vertices, then* $\lim_{n\to\infty} R^T_{max}(n) = \frac{1}{2^d}\lim_{n\to\infty} R^L_{max}(n)$*, where* R^T_{max} *is the maximum effective resistance between any two vertices in a d-dimensional toroidal graph.*

The case $d = 1$ corresponds to a network distributed over a line graph, which we now examine further.

Example (Line graph)**.** Here we examine in more detail the second order oscillator network with local damping for the case $d = 1$. If, as in Example 5.2.1, we pick i and j to be the two end vertices of the graph we obtain $P_{ij} = \dfrac{1}{24\gamma}(n^3 - n)$. Therefore for large networks with $d = 1$, the upper bound gives the correct order of the growth of P_{ij}.

If instead of considering the coherence of the whole network, we want to measure just the coherence of some subnetwork consisting of p consecutive oscillators, we can pick i and j to be the oscillators at either end of the desired subset. In this case, $P_{ij} = \dfrac{1}{4\gamma}\left(-\dfrac{1}{3}R^3_{ij} + \dfrac{1}{2}nR^2_{ij} + \dfrac{1}{3}R_{ij}\right)$. This demonstrates that for the local damping case, the performance of a subset of the network (e.g. the part between i and j), can depend on the properties of the rest of the network. This is not the case for oscillator networks with global damping.

Example (Complete graph)**.** Consider an oscillator network whose underlying graph is an n vertex complete graph with unit edge weights. The effective resistance between any two vertices is $R_{Bij} = \frac{2}{n}$. Hence for a first order oscillator network $P_{ij} = \frac{1}{2}R_{Bij} = \frac{1}{n}$, and for a second order oscillator network with global damping $P_{ij} = \frac{1}{2\beta}R_{Bij} = \frac{1}{\beta n}$. For a second order oscillator network with local damping such that $L_D = \gamma L_B$, $P_{ij} = \frac{1}{4\gamma}R^2_{Bij} = \frac{1}{n^2\gamma}$. In this case the lower bound given by Theorem 7 is $\frac{1}{n^2\gamma} \leq P_{ij}$, and the upper bound from Theorem 6 is $P_{ij} \leq \frac{2}{n\gamma}$. Observe that is this case the lower bound from Theorem 7 is exact.

The proceeding examples show our effective resistance based results applied to networks whose underlying graphs have very different connectivities.

5.3 A Simple Case of Effective Resistance

We now present one result about effective resistance. Specifically, we show that when two vertices in a graph are connected by a single path, the effective resistance between the two vertices is given by the sum of the reciprocals of the edge weights along the path. This notion is formalized in the following theorem which was previously presented in [22].

Theorem 9. *Consider a graph, $\mathcal{G} = \{\mathcal{V}, \mathcal{E}, \mathcal{W}\}$. Let L denote its weighted graph Laplacian. Let $p_1, p_{m+1} \in \mathcal{V}$, $p_1 \neq p_{m+1}$. If there is only one path,*

$$\mathcal{P} = (p_1, p_2, \ldots, p_m, p_{m+1}),$$

between p_1 and p_{m+1}, then

$$\left(\mathbf{e}_{p_1} - \mathbf{e}_{p_{m+1}}\right)^\intercal L^\dagger \left(\mathbf{e}_{p_1} - \mathbf{e}_{p_{m+1}}\right) = \sum_{k=1}^{m} \frac{1}{\mathcal{W}\left(\{p_k, p_{k+1}\}\right)}.$$

Proof. Let $\mathcal{G}'$ be an orientation of $\mathcal{G}$ such that $(p_k, p_{k+1}) \in \mathcal{E}'$, $\forall 1 \leq k \leq m$. Let $M \in \mathbb{R}^{|\mathcal{E}| \times |\mathcal{V}|}$ be an oriented and weighted (see Section 2.3) incidence matrix of $\mathcal{G}$. Partition M as $M = \begin{bmatrix} M_1^\intercal & M_2^\intercal \end{bmatrix}^\intercal$ such that $M_1 \in \mathbb{R}^{m \times |\mathcal{V}|}$ corresponds exactly to the edges traversed by $\mathcal{P}$ and the k^{th} row of M_1 corresponds to $(p_k, p_{k+1}) \in \mathcal{E}'$.

First we show that $\mathcal{R}\left(M_1^\intercal\right) \cap \mathcal{R}\left(M_2^\intercal\right) = \{0\}$. Suppose that $\mathcal{R}\left(M_1^\intercal\right) \cap \mathcal{R}\left(M_2^\intercal\right) \neq \{0\}$. Then $\exists \mathbf{v} \in \mathbb{R}^{|\mathcal{E}|}$ with $[v]_k = 0$, and some $\mathbf{x} \in \mathbb{R}^{|V|}$ the k^{th} row of M_1, such that $\mathbf{x}^\intercal = \mathbf{v}^\intercal M$. Therefore there exists some cycle that includes the two vertices that are the endpoints of the edge corresponding to the k^{th} row of M_1. This implies that there are two paths from p_1 to p_{m+1}, and hence by contradiction, $\mathcal{R}\left(M_1^\intercal\right) \cap \mathcal{R}\left(M_2^\intercal\right) = \{0\}$.

Let $\mathbf{v} \in \mathbb{R}^m$ be defined by

$$[\mathbf{v}]_k = \frac{1}{\sqrt{\mathcal{W}\left(\{p_k, p_{k+1}\}\right)}}. \tag{5.11}$$

Observe that

$$M_1 \mathbf{v} = M^\intercal \begin{bmatrix} \mathbf{v} \\ 0 \end{bmatrix} = \mathbf{e}_{p_1} - \mathbf{e}_{p_{m+1}}. \tag{5.12}$$

Therefore

$$\left(\mathbf{e}_{p_1} - \mathbf{e}_{p_{m+1}}\right)^\intercal L^\dagger \left(\mathbf{e}_{p_1} - \mathbf{e}_{p_{m+1}}\right) = \|\left(\mathbf{e}_{p_1} - \mathbf{e}_{p_{m+1}}\right)^\intercal M^\dagger\|_F^2 = \|\begin{bmatrix}\mathbf{v}^\intercal & 0\end{bmatrix} MM^\dagger\|_F^2. \tag{5.13}$$

$\mathcal{R}\left(M_1^\intercal\right) \cap \mathcal{R}\left(M_2^\intercal\right) = \{0\}$ implies that [27]

$$MM^\dagger = \begin{bmatrix} M_1 M_1^\dagger & 0 \\ 0 & M_2 M_2^\dagger \end{bmatrix}.$$

The subgraph described by M_1 is acyclic, and hence $\mathcal{N}\left(M_1^\intercal\right) = \{0\}$. Therefore rank $M_1^\intercal = m$,[1] which implies that $M_1 M_1^\dagger = I$, and hence

$$\left(\mathbf{e}_{p_1} - \mathbf{e}_{p_{m+1}}\right)^\intercal L^\dagger \left(\mathbf{e}_{p_1} - \mathbf{e}_{p_{m+1}}\right) = \|\mathbf{v}\|_2^2.$$

Clearly, $\|\mathbf{v}\|_2^2 = \sum_{k=1}^{m} \frac{1}{\mathcal{W}(\{p_k, p_{k+1}\})}$, which completes our proof. □

Remark 9. *Theorem 9 is an intuitive result because*

$$R_{p_1, p_{m+1}} = \left(\mathbf{e}_{p_1} - \mathbf{e}_{p_{m+1}}\right)^\intercal L^\dagger \left(\mathbf{e}_{p_1} - \mathbf{e}_{p_{m+1}}\right) \tag{5.14}$$

is the effective resistance between p_1 and p_{m+1} in $\mathcal{G}$. The effective resistance is the resistance between two nodes in the resistor network described by $\mathcal{G}$, where the edge weights are the conductances of each resistor in the network [16]. Therefore Lemma

[1] R. Diestel [28] proves this condition for an analogous oriented incidence matrix. An similar proof holds for the weighted, oriented, incidence matrix here because rank is invariant under row operations.

9 can be thought of as a generalization of the expression for the equivalent resistance of resistors in series.

Theorem 9 allows us to use Theorems 5, 6, and 7 to investigate the nodal performance of two oscillators connected by a single path. Specifically, for second order oscillator networks with global damping, the nodal performance of any pair of nodes connected by a single path is entirely determined by the properties along the path, and does not depend on the rest of the network. This is not the case for oscillator networks with local damping, where the properties of the network outside of the part of the network between the two nodes can affect the the nodal performance.

Chapter 6

Applications

In this chapter we show how the results of Chapter 5 can be applied to two areas of interest. First we consider power grids and investigate the transient resistive power losses due to maintaining synchrony in the face of disturbances. We then examine vehicle platoons and show how the structure of the vehicles' local control laws can affect the coherence of the platoon.

6.1 Power Grids

In this section we model the dynamics of a power grid consisting of synchronous generators coupled by lines as an oscillator network. We first present the full nonlinear dynamics of the power grid, and then linearize the dynamics about a stable operating point in order to evaluate the performance. The linearized dynamics are a second order oscillator network with local damping, and therefore we apply the results of Chapter 5. We introduce the concept of the effective line ratio, and provide interesting results for the case of equal effective line ratios. We then present some bounds on the network performance when the line ratios are not equal. Numerical simulations that illustrate the theory are also presented.

6.1.1 Nonlinear network dynamics

We consider n synchronous generators connected by lines modeled as circuit elements with susceptance, b_{ij}, and conductance, g_{ij}. The network can be represented as two weighted graphs, $\mathcal{B} = (\mathcal{V}, \mathcal{E}, \mathcal{W}_B)$ and $\mathcal{G} = (\mathcal{V}, \mathcal{E}, \mathcal{W}_G)$, where $\mathcal{V} = \{1, \ldots, n\}$, $b_{ij} = \mathcal{W}_B(\{i,j\}), \forall \{i,j\} \in \mathcal{E}$, and $g_{ij} = \mathcal{W}_B(\{i,j\}), \forall \{i,j\} \in \mathcal{E}$. Each synchronous generator has dynamics given by

$$m_i \ddot{\theta}_i + \beta_i \dot{\theta}_i = P_{m,i} - P_{e,i} + \mathrm{w}_i, \tag{6.1}$$

where $m_i > 0$, $\beta_i > 0$, and $\theta_i \in [0, 2\pi)$ are respectively the inertia, damping, and voltage angle of the i^{th} generator. w_i is an exogenous disturbance acting on generator i. $P_{m,i}$ is the constant mechanical power input to the generator, and $P_{e,i}$ is the real electrical power injected into the power grid at node i. $P_{e,i}$ is given by [29]

$$P_{e,i} = \sum_{\{i,j\} \in \mathcal{E}} b_{ij} |V_i||V_j| \sin(\theta_i - \theta_j) + \sum_{\{i,j\} \in \mathcal{E}} g_{ij} |V_i||V_j| \cos(\theta_i - \theta_j). \tag{6.2}$$

We make the following simplifying assumptions.

1. The generators have uniform interia and damping, i.e. $m_i = m, \forall i \in \mathcal{V}$ and $\beta_i = \beta, \forall i \in \mathcal{V}$.

2. The generator voltages have uniform and constant magnitude, i.e. $|V_i| = 1, \forall i \in \mathcal{V}$.

Under these assumptions we can write the nonlinear power grid dynamics in state space form as

$$\begin{bmatrix} \dot{\boldsymbol{\theta}} \\ \ddot{\boldsymbol{\theta}} \end{bmatrix} = \begin{bmatrix} \dot{\boldsymbol{\theta}} \\ M^{-1}\left(-B\dot{\boldsymbol{\theta}} + \mathbf{P}_m - \mathbf{P}_e\right) \end{bmatrix} + \begin{bmatrix} 0 \\ M^{-1} \end{bmatrix} \mathbf{w}, \tag{6.3}$$

where $[\boldsymbol{\theta}]_i :== \theta_i$, $[\mathbf{P}_e]_i := P_{e,i}$, $[\mathbf{P}_m] := P_{m,i}$, and $[\mathbf{w}]_i := \mathrm{w}_i$. M and B are respectively given by $M := \operatorname{diag}(m\mathbf{1})$ and $B := \operatorname{diag}(\beta\mathbf{1})$.

6.1.2 Linearized network dynamics

In order to analyze the synchronization performance of the power grid, we linearize (6.3) about a stable operating point, $\begin{bmatrix} \boldsymbol{\theta}* \\ 0 \end{bmatrix}$. We will assume that $\begin{bmatrix} \boldsymbol{\theta}* \\ 0 \end{bmatrix}$ is a Lyapunov stable equilibrium point of (6.3). Let $\mathbf{x} = \boldsymbol{\theta} - \boldsymbol{\theta}^*$. The linearized dynamics are given by

$$\begin{bmatrix} \dot{\mathbf{x}} \\ \ddot{\mathbf{x}} \end{bmatrix} = \begin{bmatrix} 0 & I \\ -M^{-1}\frac{\partial \mathbf{P}_e}{\partial \boldsymbol{\theta}}\Big|_{\boldsymbol{\theta}^*} & -M^{-1}B \end{bmatrix} \begin{bmatrix} \mathbf{x} \\ \dot{\mathbf{x}} \end{bmatrix} + \begin{bmatrix} 0 \\ I \end{bmatrix} \mathbf{w}. \tag{6.4}$$

If we compute the $\frac{\partial \mathbf{P}_e}{\partial \boldsymbol{\theta}}\Big|_{\boldsymbol{\theta}^*}$ term of (6.4), we find that

$$\frac{\partial \mathbf{P}_e}{\partial \boldsymbol{\theta}}\bigg|_{\boldsymbol{\theta}^*} = \overline{L}, \tag{6.5}$$

where $\overline{L}$ is the weighted graph Laplacian of $\overline{\mathcal{B}} = \left(\mathcal{V}, \mathcal{E}, \overline{\mathcal{W}}\right)$. Here

$$\overline{\mathcal{W}}\left(\{i,j\}\right) := \cos\left(\theta_i^* - \theta_j^*\right)\mathcal{W}_B\left(\{i,j\}\right) + \sin\left(\theta_i^* - \theta_j^*\right)\mathcal{W}_G\left(\{i,j\}\right),\ \forall \{i.j\} \in \mathcal{E}. \tag{6.6}$$

This amounts to taking as our edge weight the sum of the edge weights in $\mathcal{B}$ and $\mathcal{G}$ scaled by the slope of the coupling functions $\sin(\cdot)$ and $\cos(\cdot)$.

The linearized dynamics of the power grid about the equilibrium point $(\boldsymbol{\theta}^*, 0)$ are therefore given by

$$\begin{bmatrix}\dot{\mathbf{x}}\\ \ddot{\mathbf{x}}\end{bmatrix} = \begin{bmatrix}0 & I\\ -M^{-1}\overline{L} & -M^{-1}B\end{bmatrix}\begin{bmatrix}\mathbf{x}\\ \dot{\mathbf{x}}\end{bmatrix} + \frac{1}{m}\begin{bmatrix}0\\ I\end{bmatrix}\mathbf{w}. \tag{6.7}$$

Sufficient conditions for Lyapunov stability of (6.7) are that $\overline{\mathcal{W}}_B\left(\{i,j\}\right) + \overline{\mathcal{W}}_G\left(\{i,j\}\right) \geq 0,\ \forall \{i,j\} \in \mathcal{E}$.

6.1.3 Resistive losses

We now consider the performance measure we will use to measure the synchronization performance of the power grid. Specifically we analyze the resistive losses in the power grid that are due disturbances applied to the generators. When the generators are perturbed from their synchronous state by stochastic disturbances, their voltage angles will fluctuate about $\boldsymbol{\theta}^*$. The additional power that is passed between the generators due to the difference between $\boldsymbol{\theta}$ and $\boldsymbol{\theta}^*$ will induce additional resistive losses in the lines above those that occur at synchrony. We estimate these losses by a second order approximation about $\boldsymbol{\theta}^*$ as follows. Let $\begin{bmatrix}\theta^*\\0\end{bmatrix}$ be the stable equilibrium point about which we wish to analyze the performance of the power grid. The resistive losses on the line connecting the i^{th} and j^{th} node is given by

$$P_{ij}^l = g_{ij}|V_i - V_j|^2.$$

Writing $V_i = |V_i|\sin(\theta_i^* + x_i) + \mathbf{j}|V_i|\cos(\theta_i^* + x_i)$, and by making use of our assumption that $|V_i| = 1$, $\forall i \in \mathcal{V}$ as well as standard trigonometric identities we obtain

$$P_{ij}^l = g_{ij}\left(2 - 2\cos\left(\theta_i^* + x_i - \theta_j^* - x_j\right)\right).$$

Taking the second order Taylor series expansion of P_{ij}^l about $\left(\theta_i^*, \theta_j^*\right)$ we get the following approximation.

$$P_{ij}^l \approx \tilde{P}_{ij}^l := P_{ij}^* + g_{ij}\left(2\sin\left(\theta_i^* - \theta_j^*\right)(x_i - x_j) + \cos\left(\theta_i^* - \theta_j^*\right)(x_i - x_j)^2\right), \tag{6.8}$$

where P^*_{ij} is the resistive power loss across the line when $\boldsymbol{\theta} = \boldsymbol{\theta}^*$, i.e. $x_i = x_j = 0$, $\forall i, j \in \mathcal{V}$. The total resistive power loss in the network is given by

$$P^l = \sum_{\{i,j\} \in \mathcal{E}_G} P^l_{ij},$$

which can be approximated using (6.8) as

$$P^l \approx \tilde{P}^l := P^{l*} + \sum_{\{i,j\} \in \mathcal{E}_G} g_{ij} \left(2 \sin\left(\theta_i^* - \theta_j^*\right)(x_i - x_j) + \cos\left(\theta_i^* - \theta_j^*\right)(x_i - x_j)^2\right), \tag{6.9}$$

where $P^{l*} := \sum_{\{i,j\} \in \mathcal{E}_G} P^*_{ij}$ is the total resistive power loss when $x_i = 0$, $\forall i \in \mathcal{E}_G$.

We can rewrite (6.9) as

$$\tilde{P}^l = P^{l*} + \mathbf{x}^\intercal \overline{L}_G \mathbf{x} + 2 \sum_{\{i,j\} \in \mathcal{E}_G} g_{ij} \sin\left(\theta_i^* - \theta_j^*\right)(x_i - x_j), \tag{6.10}$$

where $\overline{L}_G$ is the weighted graph Laplacian of $\overline{\mathcal{G}} = \left(\mathcal{V}, \mathcal{E}, \overline{\mathcal{W}}_G\right)$. Here

$$\overline{\mathcal{W}}_G(\{i,j\}) = \cos\left(\theta_i^* - \theta_j^*\right) \mathcal{W}_G(\{i,j\}), \forall \{i.j\} \in \mathcal{E}. \tag{6.11}$$

6.1.4 Power grid performance

We now apply the results of Chapter 5 to evaluate the mean steady state resistive losses due to maintaining synchrony in a power grid.

We define the linear input-output system, G, with dynamics given by (6.7) and an output, $\mathbf{y}$, such that $\mathbf{y}^\intercal\mathbf{y} = \mathbf{x}^\intercal\overline{L}_G\mathbf{x}$ as

$$G := \left(\begin{array}{c|c} A & \begin{bmatrix} 0 \\ I \end{bmatrix} \\ \hline \overline{L}_G^{\frac{1}{2}} & 0 \end{array}\right). \tag{6.12}$$

$\overline{L}_G^{\frac{1}{2}}$ will exist under the assumption that $\overline{\mathcal{W}}_G \geq 0$, and A is given by

$$A = \begin{bmatrix} 0 & I \\ -M^{-1}\overline{L} & -M^{-1}B \end{bmatrix}. \tag{6.13}$$

Now consider applying independent, unit strength white Gaussian noise as the input to G. In this case the steady state expected resistive losses will be

$$\lim_{t\to\infty} E\left[P^l\right] = \lim_{t\to\infty} E\left[P^{l*} + \mathbf{x}^\intercal\overline{L}_G\mathbf{x} + 2\sum_{\{i,j\}\in\mathcal{E}_G} g_{ij}\sin\left(\theta_i^* - \theta_j^*\right)(x_i - x_j)\right], \tag{6.14}$$

$$\lim_{t\to\infty} E\left[P^l\right] = P^{l*} + \lim_{t\to\infty} E\left[\mathbf{x}^\intercal\overline{L}_G\mathbf{x}\right], \tag{6.15}$$

$$\lim_{t\to\infty} E\left[P^l\right] = P^{l*} + \|G\|_{\mathcal{H}_2}^2. \tag{6.16}$$

Here we have used the fact that when the input to a linear system is zero mean Gaussian noise the states will have zero mean, and hence the term that is linear in $\mathbf{x}$ vanishes inside the expectation operator. Because we are interesting in the component of P^l that is due to resynchronization, we can ignore P^{l*} and simply compute $\|G\|_{\mathcal{H}_2}^2$.

Theorem 10. *Consider a power grid with dynamics given by* (6.3)*, where* $\mathbf{w}$ *is a vector of unit strength, independent Gaussian white noise. If the operating point* $\boldsymbol{\theta}^*$ *is The steady state expectation of the linear quadratic estimate,* $\tilde{P}^l$*, of the of the resistive losses is given by*

$$\lim_{t\to\infty} E\left[\tilde{P}^l\right] = P^{l*} + \frac{1}{2\beta}\mathrm{tr}\left(\overline{L}^{\dagger}\overline{L}_G\right) \tag{6.17}$$

Proof. The desired results follows immediately from Theorem 4 and equation (6.16).

□

We now consider a special case where a simple expression for $\tilde{P}^l$ holds. In order to do this we make the following definition.

Definition 5. Consider a power grid with dynamics given by (6.3) and an asymptotically stable equilibrium point, $\begin{bmatrix}\theta^* \\ 0\end{bmatrix}$. The generalized line ratio of the line connecting nodes i and j is defined as

$$\overline{\alpha}_{ij} := \frac{\cos\left(\theta_i^* - \theta_j^*\right)\mathcal{W}_G\left(\{i,j\}\right)}{\left(\cos\left(\theta_i^* - \theta_j^*\right)\mathcal{W}_B\left(\{i,j\}\right) + \sin\left(\theta_i^* - \theta_j^*\right)\mathcal{W}_G\left(\{i,j\}\right)\right)} \tag{6.18}$$

The following corollary of Theorem 10 gives a simple expression for $\tilde{P}^l$ that holds in the special case of equal generalized line ratios.

Corollary 1. Consider a power grid with under the conditions of Theorem 10 where $\exists\alpha \in \mathbb{R}_+$ such that

$$\overline{\alpha}_{ij} = \overline{\alpha}, \forall\{i.j\} \in \mathcal{E}. \tag{6.19}$$

In this special case Theorem 10 reduces to

$$\lim_{t\to\infty} E\left[\tilde{P}^l\right] = P^{l*} + \frac{1}{2\beta}\overline{\alpha}\,(n-1)\,. \tag{6.20}$$

Proof. The proof follows from Theorem 10 and the fact that $L_B^\dagger L_B = I - \frac{1}{n}J$. □

We refer to the conditions described in Corollary 1 as "equal generalized line ratios". Corollary 1 is a generalization of a result given by Bamieh and Gayme [20]. Bamieh and Gayme showed that Corollary 1 holds in the special case $\boldsymbol{\theta}^* = 0$, in which case condition (6.19) reduces to $\alpha = \overline{\alpha} = \frac{b_{ij}}{g_{ij}}, \forall \{i,j\} \in \mathcal{E}$ which is called equal line ratios. In the case of equal generalized line ratios, the resistive losses in the network do not depend on network structure. This is important because it implies that if the number of generators is fixed, changing the network structure cannot change the resistive losses due to maintaining synchrony.

We now derive bounds on $\tilde{P}^l$ when the generalized line ratios may not be equal. Since

$$\overline{L}_G = \sum_{\{i,j\}\in\mathcal{E}} \overline{g}_{ij}\,(\mathbf{e}_i - \mathbf{e}_j)\,(\mathbf{e}_i - \mathbf{e}_j)^\intercal\,, \tag{6.21}$$

we can use Theorem 10 to obtain

$$\lim_{t\to\infty} E\left[\tilde{P}^l\right] = P^{l*} + \frac{1}{2\beta}\sum_{\{i,j\}\in\mathcal{E}} \overline{g}_{ij} R_{\overline{B}ij}. \tag{6.22}$$

Here $R_{\overline{B}ij}$ is the effective resistance between i and j in $\overline{\mathcal{B}}$. (6.22) immediately leads to the following two pairs of bounds on $\lim_{t\to\infty} E\left[\tilde{P}^l\right]$.

$$P^{l*} + \frac{1}{2\beta}\overline{g}_{ij}^{min} R_{sum} \leq \lim_{t\to\infty} E\left[\tilde{P}^l\right] \leq P^{l*} + \frac{1}{2\beta}\overline{g}_{ij}^{max} R_{sum}$$
$$P^{l*} + \frac{1}{2\beta}R_{\overline{B}ij}^{min} \sum_{\{i,j\}\in\mathcal{E}} \overline{g}_{ij} \leq \lim_{t\to\infty} E\left[\tilde{P}^l\right] \leq P^{l*} + \frac{1}{2\beta}R_{\overline{B}ij}^{max} \sum_{\{i,j\}\in\mathcal{E}} \overline{g}_{ij}$$

where $\overline{g}_{ij}^{min} = \min_{\{i,j\}\in\mathcal{E}} \overline{g}_{ij}$, $\overline{g}_{ij}^{max} = \max_{\{i,j\}\in\mathcal{E}} \overline{g}_{ij}$, $R_{\overline{B}ij}^{min} = \min_{\{i,j\}\in\mathcal{E}} R_{\overline{B}ij}$, $R_{\overline{B}ij}^{max} = \max_{\{i,j\}\in\mathcal{E}} R_{\overline{B}ij}$, and $R_{sum} = \sum_{\{i,j\}\in\mathcal{E}} R_{\overline{G}ij}$.

In the special case where $\mathcal{B}$ and $\mathcal{G}$ are acyclic, $R_{ij} = \frac{1}{b_{ij}}$, $\forall \{i,j\} \in \mathcal{E}$. In this case,

$$\lim_{t\to\infty} E\left[\tilde{P}^l\right] = \frac{1}{2\beta} \sum_{\{i,j\}\in\mathcal{E}} \frac{\overline{g}_{ij}}{\overline{b}_{ij}}. \tag{6.24}$$

This result is particularly applicable to distribution systems, which are typically trees.

6.1.5 Simulations

The accuracy of the bounds based on $R_{\overline{B}ij}^{max}$ and $R_{\overline{B}ij}^{min}$ will vary depending on the structure of $\mathcal{B}$. To illustrate this we simulate a series of networks with the same number of oscillators, but different connections between them. Specifically, we simulate seven oscillator networks with the underlying graphs shown in Figure 6.1, ranging from a line graph to a complete graph. We use $m = 0.053$, $\beta = 0.027$, and b_{ij} and g_{ij} values drawn uniformly from respectively $[4.37, 4.47]$ and $[1.61, 1.66]$. Here we consider the performance about the operating point $\boldsymbol{\theta}^* = 0$.

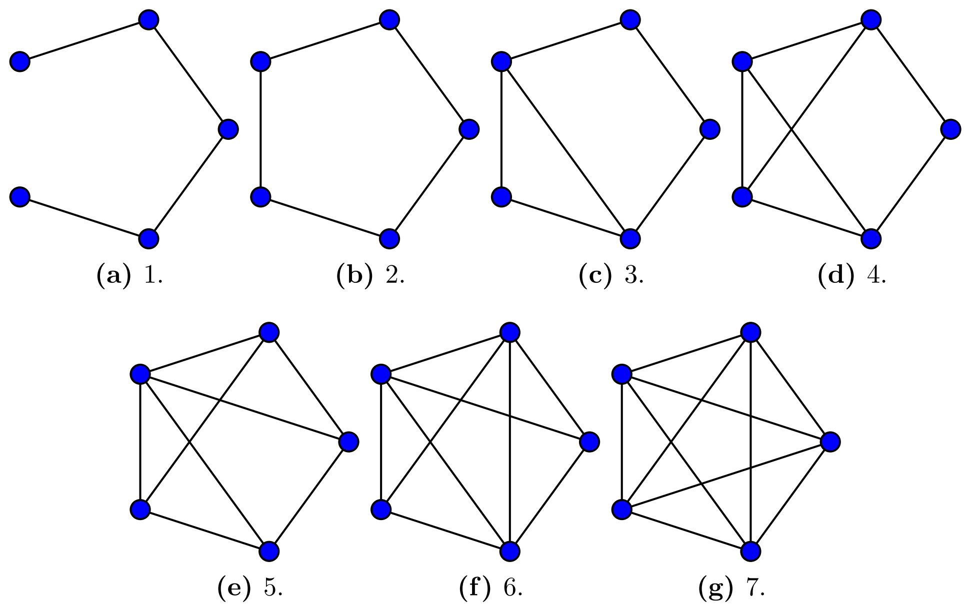

Figure 6.1: Graphs underlying simulated power grids.

Figure 6.2 shows the transient power losses and bounds based on $R_{\overline{B}ij}^{min}$, $R_{\overline{B}ij}^{max}$, $\overline{g}_{ij}^{min}$ and $\overline{g}_{ij}^{max}$ when the disturbances are independent unit strength Gaussian white noise. The bounds based on $\overline{g}_{ij}^{min}$ and $\overline{g}_{ij}^{max}$ are better than the effective resistance based bounds in this case. This is because the spread of $\overline{g}_{ij}$ values is relatively small, but for many of the graphs the range of effective resistances is relatively large due to the effective resistance being determined by graph structure as well as line weights.

6.2 Vehicle Platoons

One application area where the results of Section 5.2 are useful is vehicle platoons. A vehicle platoon consists of a set of n vehicles, each of which uses a feedback control law in an attempt to maintain some nominal spacing with its neighbors. The struc-

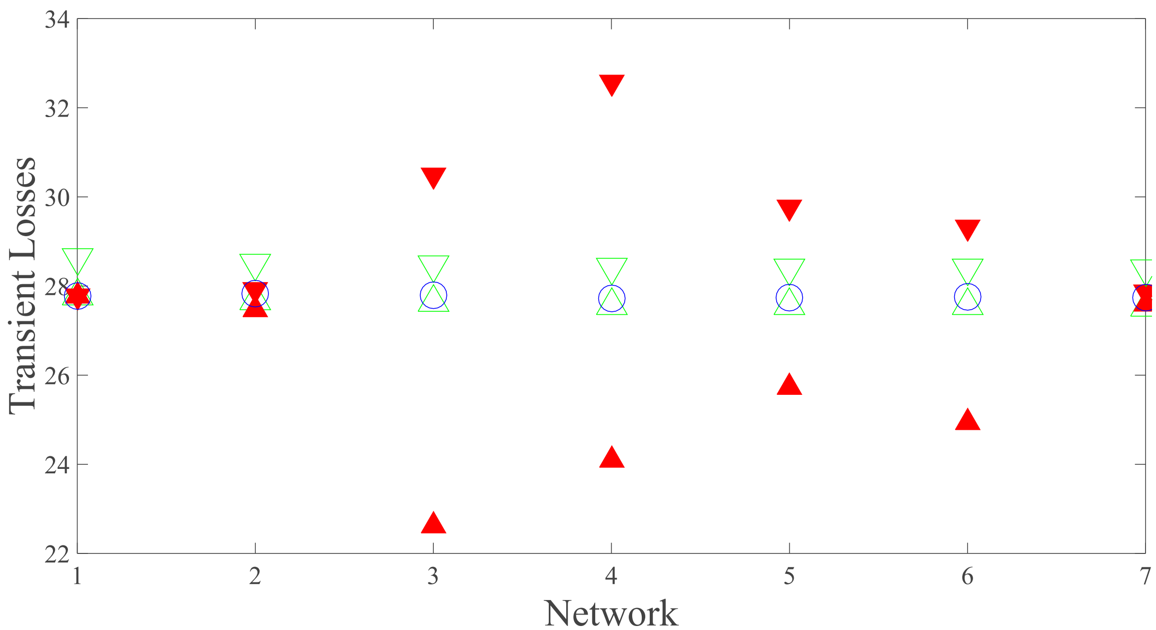

Figure 6.2: Expected transient power losses and bounds for seven different power grids with five generators. ◯ denotes the true value of the expected transient losses, △ [▽] denotes the lower [upper] bound based on $\bar{g}_{ij}^{min}$ [$\bar{g}_{ij}^{max}$], and ▲ [▼] denotes the lower [upper] bound based on $R_{\overline{B}ij}^{min}$ [$R_{\overline{B}ij}^{max}$].

ture of the platoon is described by an unweighted graph, $\Gamma = (\mathcal{V}, \mathcal{E})$, with vertices corresponding to vehicles and edges determining which vehicles are adjacent to each other. The dynamics of each vehicle are given by

$$m\ddot{x}_i = \mathrm{w}_i + u_i,$$

where m, w_i, and u_i are respectively the inertia, disturbance, and control input at the i^{th} vehicle. x_i is the deviation of the i^{th} vehicle from its nominal position. u_i is determined by a control law which computes u_i based on x_i as well as x_j, $\forall j \sim i$. We consider the following two control laws.

6.2.1 Local position and absolute velocity control

Here each vehicle adjusts its position based on the difference between its position and that of its neighbors, as well as its velocity. In this control scheme each vehicle must posses a method of determining the distance to its neighbors as well as a method for determining its velocity relative to some reference that all the vehicles share. In this case,

$$u_i = -b \sum_{\{i,j\} \in \mathcal{E}} (x_i - x_j) - \beta \dot{x}_i,$$

where b and β are two parameters. Let L_Γ be the weighted graph Laplacian of Γ, then the closed loop dynamics of the system under this control law are exactly (3.3) with $L_B = bL_\Gamma$, i.e. an oscillator network with global damping.

6.2.2 Local position and local velocity control

Here u_i depends on the position of the i^{th} vehicle relative to its neighbors, and on the velocity of the i^{th} vehicle relative to its neighbors. In this case,

$$u_i = -b \sum_{j \sim i} (x_i - x_j) - d \sum_{j \sim i} (\dot{x}_i - \dot{x}_j),$$

where d is some parameter. The closed loop dynamics of the system under this control law are precisely (3.4) with $L_B = bL_\Gamma$ and $L_D = dL_\Gamma$, i.e. an oscillator network with local damping.

We measure the performance of the vehicle platoon in terms of the coherence, or how much the platoon acts like a solid object. We will quantify the coherence in terms of the long range disorder, i.e.

$$P_{ij} = \lim_{t \to \infty} E\left[(x_i - x_j)^2\right],$$

where i and j are chosen to be "far apart" in the platoon. As we will see, the correct notion of far apart is to pick i and j such that $\{i, j\} = argmax_{\{i,j\} \in \mathcal{E}} R_{\Gamma ij}$. The results of Section 5.2 tell us that for the platoon using control law 1,

$$P_{ij} = \frac{1}{2b\beta} R_{\Gamma ij},$$

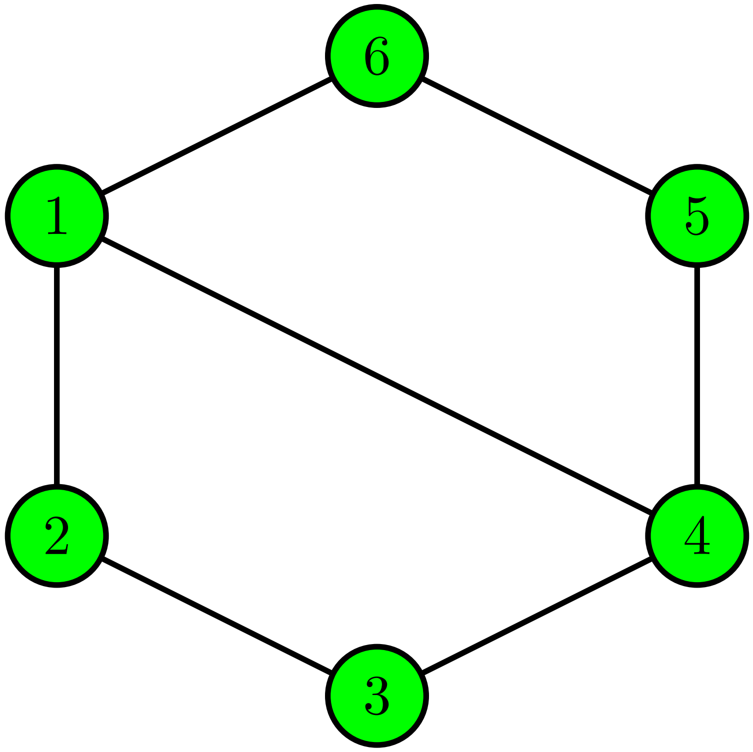

Figure 6.3: The graph, $\mathcal{B}$, underlying the simulated vehicle platoon for $n = 6$. In this case the long range disorder is measured by P_{25} (or equivalently P_{36}) since R_{B25} is the maximum effective resistance in $\mathcal{B}$.

whereas for the platoon using control law 2,

$$\frac{1}{4bd} R^2_{\Gamma ij} \leq P_{ij} \leq \frac{n}{2bd} R^2_{\Gamma ij}.$$

The long range disorder in the platoon therefore scales with $R^{max}_{\Gamma ij}$ when control law 1 is used, and between $\left(R^{max}_{\Gamma ij}\right)^2$ and $n \left(R^{max}_{\Gamma ij}\right)^2$ when control law 2 is used.

In order to illustrate these results we simulate a series of vehicle platoons that increase in size while maintaining the same structure. Specifically, we simulate vehicle platoons arranged in a circle with an additional edge running across the middle. The

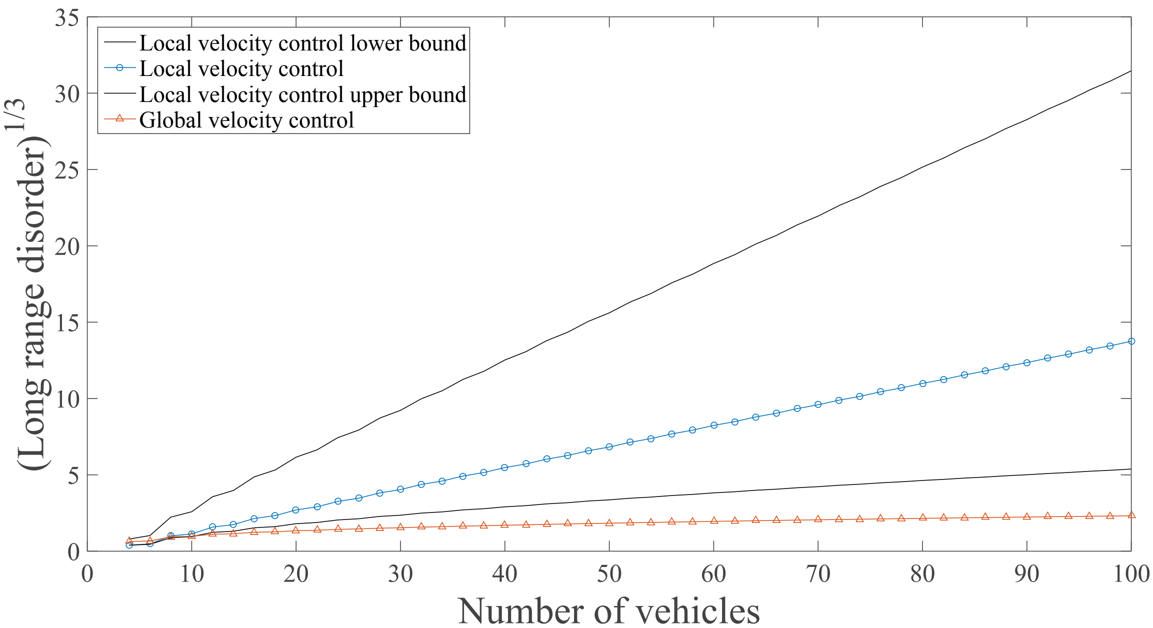

Figure 6.4: Cube root of long range disorder v.s. platoon size in vehicle platoons with local position control and either absolute (control law 1) or local (control law 2) velocity control. The long range disorder is measured by P_{ij} where $\{i, j\}$ is chosen to maximize $R_{\Gamma ij}$. To preserve symmetry only even numbers of vehicles are simulated.

graph that represents such an arrangement is shown for $n = 6$ in Figure 6.3. For simplicity we use $b = d = \beta = m = 1$ as our parameters. The results of using control laws 1 and 2 as well as the bounds for the performance of the platoon using control law 2. It can be seen from the plot that asymptotically, the order of the upper bound for control law 2 is the same as that for the true value of the long range disorder using control law 2. The absolute velocity control platoon has better coherence for every size platoon, which indicates that for relatively sparse graph like the one considered here, absolute velocity control maintains better coherence than local velocity control.

Chapter 7

Conclusions

In this work we consider the performance of oscillator networks in terms of their steady state response to stochastic disturbances. We first present results that extend Lyapunov equation theory in order to develop simple methods to compute the observability Gramians of systems on graphs directly from the canonical non-minimal realizations. Using these results we first examine the case of a single disturbance affecting a network of locally or globally damped oscillators. In particular, we characterize how the location of the disturbance changes its effect on network coherence and the amount of interaction between the oscillators. Our results show that for oscillator networks with global damping, the location of the disturbance does not change the amount of interaction between oscillators, which is uniform and depends only on the damping constant and number of oscillators. This extends the results of Bamieh and Gayme [20], who showed that in a network with global damping the amount of interaction between oscillators due to disturbances at every oscillator depends only on the damping constant and number of oscillators. Specifically, our result shows that the contribution of each disturbance to the interaction between oscillators is uniform. We then examine the case of disturbances applied at every oscillator in the network. In this case we connect the nodal performance of pair of oscillators in the network to the effective resistance in the underlying graph between those oscillators. The nodal performance measures the coherence of the subnetwork connecting the two chosen oscillators. Additionally, a large class of performance measures can be constructed from the nodal performances of every pair of oscillators in the network. We give exact results for oscillator networks with global damping and provide upper and lower bounds for networks with local damping. One application of our results is analyzing the coherence of platoons of vehicles with local and absolute velocity feedback.

Bibliography

[1] P. Barooah and J. Hespanha, "Error amplification and disturbance propagation in vehicle strings with decentralized linear control," in *Proc. 44^{th} IEEE Conf. Decision and Contr.*, Orlando, FL, 2005, pp. 4964–4969.

[2] P. Seiler, A. Pant, and K. Hedrick, "Disturbance propagation in vehicle strings," *IEEE Trans. Automat. Contr.*, vol. 49, no. 10, pp. 1835–1842, Oct. 2004.

[3] H. Hao and P. Barooah, "Stability and robustness of large platoons of vehicles with double-integrator models and nearest neighbor interaction," *Int. J. Robust and Nonlinear Contr.*, vol. 23, no. 18, pp. 2097–2122, July 2013.

[4] A. E. Motter, S. A. Myers, M. Anghel, and T. Nishikawa, "Spontaneous synchrony in power-grid networks," *Nature Physics*, vol. 9, no. 3, pp. 191–197, Feb. 2013.

[5] F. Dorfler and F. Bullo, "Synchronization and transient stability in power networks and nonuniform kuramoto oscillators," *SIAM J. Contr. and Optim.*, vol. 50, no. 3, pp. 1616–1642, June 2012.

[6] A. Bergen and D. Hill, “A structure preserving model for power system stability analysis,” *IEEE Trans. Power App. Syst.*, vol. PAS-100, no. 1, pp. 25–35, Jan. 1981.

[7] F. Dorfler and F. Bullo, “Spectral analysis of synchronization in a lossless structure-preserving power network model,” in *1st IEEE Int. Conf. Smart Grid Commun.*, 2010, pp. 179–184.

[8] R. Mirollo and S. Strogatz, “Synchronization of pulse-coupled biological oscillators,” *SIAM J. Applied Math.*, vol. 50, no. 6, pp. 1645–1662, July 1990.

[9] F. Dörfler and F. Bullo, “Synchronization in complex oscillator networks: A survey,” *Automatica*, vol. 50, no. 6, pp. 1539–1564, June 2014.

[10] G. F. Young, L. Scardovi, and N. E. Leonard, “Robustness of noisy consensus dynamics with directed communication,” in *Proc. American Contr. Conf.*, Baltimore, MD, 2010, pp. 6312–6317.

[11] M. Siami and N. Motee, “Fundamental limits on robustness measures in networks of interconnected systems,” in *Proc. 52nd IEEE Conf. Decision and Contr.*, Florence, Italy, 2013, pp. 67–72.

[12] E. Tegling, B. Bassam, and D. F. Gayme, “The price of synchrony: evaluating the resistive losses in synchronizing power networks,” *IEEE Trans. Contr. Netw. Syst.*, 2015, to Appear.

[13] F. Dorfler, M. Jovanović, M. Chertkov, and F. Bullo, "Sparsity-promoting optimal wide-area control of power networks," *IEEE Trans. Power Syst.*, vol. 29, no. 5, pp. 2281–2291, Sept. 2014.

[14] F. Lin, M. Fardad, and M. Jovanović, "Optimal control of vehicular formations with nearest neighbor interactions," *IEEE Trans. Automat. Contr.*, vol. 57, no. 9, pp. 2203–2218, Sept. 2012.

[15] B. Bamieh, M. R. Jovanović, P. Mitra, and S. Patterson, "Coherence in large-scale networks: Dimension-dependent limitations of local feedback," *IEEE Trans. Automat. Contr.*, vol. 57, no. 9, pp. 2235–2249, Sept. 2012.

[16] F. Dörfler and F. Bullo, "Synchronization of power networks: Network reduction and effective resistance," in *IFAC Workshop on Distrib. Estim. and Contr. Netw. Syst.*, 2010, pp. 197–202.

[17] P. Barooah and J. P. Hespanha, "Graph effective resistance and distributed control: Spectral properties and applications," in *Proc. 45^{th} IEEE Conf. Decision and Contr.*, San Diego, CA, 2006, pp. 3479–3485.

[18] ——, "Error scaling laws for linear optimal estimation from relative measurements," *IEEE Trans. Inf. Theory*, vol. 55, no. 12, pp. 5661–5673, 2009.

[19] Q. Huang, Y. Yuan, J. Goncalves, and M. Dahleh, "H2 norm based network

volatility measures," in *Proc. American Contr. Conf.*, Portland, OR, 2014, pp. 3310–3315.

[20] B. Bamieh and D. F. Gayme, "The price of synchrony: Resistive losses due to phase synchronization in power networks," in *Proc. American Contr. Conf.*, Washington, DC, 2013, pp. 5815–5820.

[21] E. Sjödin and D. F. Gayme, "Transient losses in synchronizing renewable energy integrated power networks," in *Proc. American Contr. Conf.*, Portland, OR, 2014, pp. 5217–5223.

[22] T. W. Grunberg and D. F. Gayme, "Nodal performance measures for oscillator networks with local and global damping," in *Proc. American Contr. Conf.*, Chicago, July 2015, to Appear.

[23] T. Kailath, *Linear systems.* Prentice-Hall Upper Saddle River, NJ, 1980, vol. 1.

[24] E. Sjödin, "The price of synchrony: Evaluating transient power losses in renewable energy integrated power networks," Master's Thesis, Royal Institute of Technology, August 2014.

[25] I. Gutman and W. Xiao, "Generalized inverse of the Laplacian matrix and some applications," in *Bulletin of the Serbian Academy of Sciences and Arts*, vol. 29, 2004.

[26] R. A. Horn and C. R. Johnson, *Matrix Analysis.* New York: Cambridge university press, 2012.

[27] A. Ben-Israel and T. N. Greville, *Generalized inverses: theory and application.* Wiley-Interscience, 1974.

[28] R. Diestel, *Graph Theory* {*Graduate Texts in Mathematics; 173*}. New York: Springer-Verlag, 2000.

[29] A. von Meier, *Electric Power Systems: A Conceptual Introduction.* John Wiley & Sons, 2006.

Vita

Theodore W. Grunberg received the Bachelor of Science degree in Mechanical Engineering from the Johns Hopkins University in 2013, graduating with general and departmental honors. He received the Robert George Gerstmyer award for undergraduate achievement in mechanical engineering in 2013. From 2013 to 2015 he was a masters student in the Networked and Spatially Distributed Systems group in the Laboratory for Computational Sensing and Robotics at Johns Hopkins. His research focuses on the analysis and control of systems distributed over graphs. His publications have appeared at both the IEEE Conference on Decision and Control and the American Controls Conference.